

Article

Microclimate Thermal Management Using Thermoelectric Air-Cooling Duct System Operated at Five Incremental Powers and its Effect on Sleep Adaptation of the Occupants

Kashif Irshad ^{1,*} , Salem Algarni ², Mohammad Tauheed Ahmad ³, Sayed Ameenuddin Irfan ⁴, Khairul Habib ⁵, Mostafa A.H. Abdelmohimen ^{2,6}, Md. Hasan Zahir ¹ and Gulam Mohammed Sayeed Ahmed ² 

¹ Center of Research Excellence in Renewable Energy (CoRE-RE), King Fahd University of Petroleum & Minerals, Dhahran 31261, Saudi Arabia; hzahir@kfupm.edu.sa

² Department of Mechanical Engineering, King Khalid University, Abha 61413, Saudi Arabia; saalgarni@kku.edu.sa (S.A.); mmhussien@kku.edu.sa (M.A.H.A.); drgmsa786@gmail.com (G.M.S.A.)

³ College of Medicine, King Khalid University, Abha 61413, Saudi Arabia; combatobacco@gmail.com

⁴ Department of Fundamental and Applied Sciences, Universiti Teknologi PETRONAS, Bandar Seri Iskandar, Perak Darul Ridzuan 32610, Malaysia; slirfan7@gmail.com

⁵ Department of Mechanical Engineering, Universiti Teknologi PETRONAS, Bandar Seri Iskandar, Perak Darul Ridzuan 32610, Malaysia; khairul.habib@utp.edu.my

⁶ Mechanical Engineering Department, Shoubra Faculty of Engineering, Benha University, Cario 13511, Egypt

* Correspondence: kashif.irshad@kfupm.edu.sa

Received: 10 August 2019; Accepted: 24 September 2019; Published: 27 September 2019



Abstract: In this study, the microclimate of the test room was regulated using thermoelectric air duct cooling system (TE-AD) operated at input powers-240 W, 360 W, 480 W, 600 W, 720 W, and 840 W, on subsequent nights. Fifteen (15) healthy male volunteers were recruited to sleep under these test conditions and their sleep quality was assessed by studying objective measures such as sleep onset latency (SOL), mean skin temperature and heart rate as well as subjective parameters like predicted mean vote (PMV) and predicted percentage of dissatisfied (PPD). There was a consistent improvement on all studied parameters when the power of the system was increased from 240 W to 720 W. The mean sleep onset latency time was reduced from ($M = 40.7 \pm 0.98$ min) to ($M = 18.33 \pm 1.18$ min) when the operating power was increased from 240 W to 720 W, denoting an improvement in sleep quality. However, increasing the power further to 840 W resulted in deteriorating cooling performance of the TE-AD system leading to an increase in temperature of the test room and reduction in sleep comfort. Analysis of subjective indices of thermal comfort viz. PMV and PPD revealed that subjects are highly sensitive towards variations in microclimate achieved by changing the operating power of the TE-AD. This device was also found to be environmentally sustainable, with estimated reduction in CO₂ emission calculated to be around 38% as compared to the conventional air-conditioning.

Keywords: sleeping comfort; adaptive model; thermoelectric cooling; variable operating power; CO₂ emission

1. Introduction

Adequate sleep is important for maintaining a healthy and productive lifestyle. Impaired quality and reduced duration of sleep may lead to serious short-term and long-term health and related consequences [1]. This can range from increased risks of obesity, Type-2 diabetes to a spectrum of cardiovascular ailments [2]. Studies have also linked lack of adequate sleep to workplace injuries and

road traffic accidents [3]. Indoor thermal environment affects the sleep comfort of the occupants [4]. Quality of sleep is strongly linked to the thermal microenvironment as established by several studies [5]. Excessive environmental heat is more of a problem in tropical and sub-tropical countries [6]. In these geographic zones, where temperature and relative humidity remain high for most part of the day throughout a greater part of the year, air-conditioners are being increasingly used to provide a comfortable ambient microclimate [7]. This use of air-conditioners to adapt the indoor and built environments has increased rapidly in the past decades leading to a rise in energy consumption, and the resultant total CO₂ emissions [8]. Climate change has further aggravated the environmental heat problem by threatening the health and well-being of vulnerable populations in these areas [9]. A slight increase or decrease in the thermal environment creates a disturbance in the sleeping behavior of the occupants [10]. According to studies, chronic sleep problems in the US have been estimated to occur in up to 70 million people [11] while in Europe around 45 million people [12] have one or other chronic sleep problem. Studies estimating the sleep problem in developing countries are lacking.

However, due to lower average standards of living in the developing world and consequent lack of comfortable sleeping environment, sleep problems are suspected to be higher in developing countries. This is more so in those countries with hot and humid conditions, as researches point that thermal microclimate of the sleeping space is a major factor impacting sleep quality [13]. Sleep has been identified to happen in distinct stages: stage of rapid eye movement (REM) sleep and stage of non-rapid eye movement sleep (NREM). NREM sleep comprises of four stages, progressing in depth of sleep from Stage 1 to Stage 4. Stages 3 and 4 of the NREM are combined, and designated as slow-wave sleep (SWS). SWS has been found to provide the body with a recess for physical restoration and happens in the initial one-third of the night [14]. In contrast, the REM pattern of sleep is more in the last one-third of the sleep. Sleep starts with NREM sleep and progresses through the deeper stages of sleep (Stage 1 to Stage 4) followed by REM sleep. The sleep alternates between NREM and REM with an approximately 90 min cycle. A normal person may have 4 to 6 such episodes during a 6–7 h sleeping period. As the night progresses, the NREM stages become fewer, while the duration of REM sleep episode increases [15].

Morito et al. [14] evaluated sleeping performances of occupants under three different types of air flow from air-conditioning system. The result shows that occupants sleep did not show significant variation when air-conditioner system circulates average air flow rate at 0.14 m/s and 0.04 m/s. However, negative responses were recorded when air flow rate increased beyond 0.2 m/s. Pan et al. [16] investigates sleeping comfort of the occupants at three microclimatic temperature, i.e., 23 °C, 26 °C and 30 °C. At all three temperatures, it was found that the ratings of occupants were towards a slightly warmer side during waking state (WS) as compared to that during sleep. Recently, use of thermoelectric module (TEM) as an alternative of traditional air-conditioner system was researched and found to have many advantages such as a solid structure, reliable operation, energy efficiency, eco-friendliness and freedom from refrigerants [17,18].

Research to assess the efficiency of TEM systems to improve the thermal comfort of indoor areas during waking state as well as during sleep are in the initial stages but the findings are promising [19]. Lertsatitthanakorn et al. [20] in his experiment placed a thermoelectric ceiling cooling panel (TE-CCP) system on the ceiling of a test chamber of volume 4.5 m³ and evaluated the effect on temperature regulation and thermal comfort. An assessment of its effects on cooling and comfort performance was conducted. An enhancement in the performance of the system was achieved when water was circulated to the heat exchanger made up of the copper which was situated at the warm part of the thermoelectric module and a ceiling panel made up of aluminum was affixed to the cooler part of the TEM. At the set mean interior temperature of 27 °C and a mean air velocity of 0.8 m/s, the TE-CCP was able to achieve a cooling capacity of 201.6 W with a coefficient of performance (COP) of 0.82. On subjective evaluation more than 80 percent of the occupiers reported 'thermally satisfied' with the system meeting the American Society of Heating, Refrigerating and Air-Conditioning Engineers (ASHRAE) Standard 55 with an acceptability of 80%. Maneewan et al. [21] investigated the thermal

comfort and economic efficiency of cooling of air using TE-AD in a test chamber of area 16 m². It was found that the payback duration and energy efficiency decreased on increasing the number of TEM units. An estimated maximum electrical savings of US \$153.90 per year was achieved, with an estimated payback period of 0.75 with a one-unit TEM air-conditioner. Occupants reported 'thermally satisfied' at this configuration and the system met the ASHRAE Standard 55 [22] with a cooling capacity of 29.2 W and COP of 0.34. Lertsatitthanakorn et al. [23] in another study assessed the cooling performance and thermal microclimate modulation of a test room of volume 4.5 m³ fitted with a TE cooling device. A total of 36 TEMs were functioned at 1 A, resulting in a cooling capacity of 201.6 W and a coefficient of performance of 0.82. A comfort examination demonstrated that the subject appraisals toward the test-room microclimatic conditions fit well with ASHRAE Standard 55 [22]. Irshad et al. [24] investigated the microclimatic regulation in a test room fitted with a TE-AD device. It was found that the operating power of 6 A and 5 V produced the maximum thermal comfort. At this specification, a PMV in the range of ± 1 was obtained from more than 80% of the occupants as per ASHRAE Standard 55 specifications.

Irshad et al. [25] investigates thermal comfort of test chamber fitted with both a PV wall system and TE-AD cooling system in Malaysian climatic conditions. From the outcome of this experiment one can infer that the implementation of a PV panel and a TE-AD system on the south facing wall and north facing wall of the test chamber respectively reduced the heat load and increased thermal comfort levels inside the room. Parameters such as overall thermal sensation ratings, PMV, and PPD, concluded that occupants 'thermally satisfaction' rate increased above 90%. Kimmling et al. [26] presented a preliminary study assessing the thermal comfort of a building having PV panels that provided power to the thermoelectric cooling system which worked by radiative cooling. This system resulted in better thermal sensation and thermal comfort of the subjects.

Review of extant literature suggests a lack of study pertaining to the sleeping behavior and adaptation of occupants when they are resting inside a room-chamber consisting of a thermoelectric cooling system. This study endeavors to bridge this gap by investigating the sleeping comfort and adaptive parameters of occupants in test chamber fitted with a TE-AD cooling system in tropical climate. In this study, the subjective reportings of the occupants (before and after sleep) as well as objective findings (recorded during sleep) were evaluated at six different inputs to the TE-AD from 240 W to 840 W. A schematic illustration and the design guidelines used in this research are also provided in the relevant sections.

2. Methodology

2.1. Test Chamber

A test chamber of volume 21.16 m³, situated in the research facility of Universiti Teknologi PETRONAS, Perak, Malaysia was utilized for this experiment. The measured volume of the study test chamber was 21.16 m³. The north-side enclosure of the test room was fitted with a thermoelectric air channel cooling framework (TE-AD) with adjustable power capacity starting from 240 W to 840 W. The components of the TE-AD framework was set up as specified in a previous study [27]. The test chamber comprised of a bed of measurement (0.91 m \times 1.88 m), a wooden chair, a general-use table of measurement (1.2 m \times 0.49 m \times 0.77 m). A LED bulb (20 W, 1600 lm), and a roof fan of specifications (54 W, 330 rpm, and 200 cm³/min) were pre-fitted in the room.

2.2. Description of Occupants

A number of prospective male subjects were screened to shortlist 15 healthy participants with no histories of - recent intake of medications, any recognized sleep disorder, erratic sleep pattern, any illness which may affect sleep such as asthma, hypertension, or recent fever (Table 1). Fifteen male occupants were chosen due to extensive experimental duration and phases. As mentioned below each occupants has to spend nights in the test room for six different combination of input power supply to

the TE-AD system. Further, prior to recruitment in this study, the sleep pattern history of the past one week of the occupants was noted to exclude any subject with sleep abnormality. Before the start of the study the subjects registered their responses on the Pittsburgh Sleep Quality Index (PSQI) and subjects with a PSQI score > 5 were excluded from the study [28]. A subjective opinion of the thermal comfort was recorded from the occupants before the start of the experiment (Figure 1). The occupant characteristics had been validated in an earlier study [29]. The subject wore a sleeping dress comprising of thin trousers (0.20 clo), a short-sleeved round neck t-shirt (0.09 clo), and a thin blanket (0.32 clo) was supplied to the subjects to cover the body while sleeping. The subjects were compensated at a fixed rate and no rewards were to be given. Research ethics committee of the university approved the study.

Table 1. Anthropometric data of subjects.

Sex	Sample Size	Age	Height (m)	Mass (kg)	BMI (kg/m ²)
Male	15	28.3 \pm 4.8 *	1.69 \pm 0.07	70.2 \pm 0.7	24.3 \pm 1.7

Note: * Standard Deviation

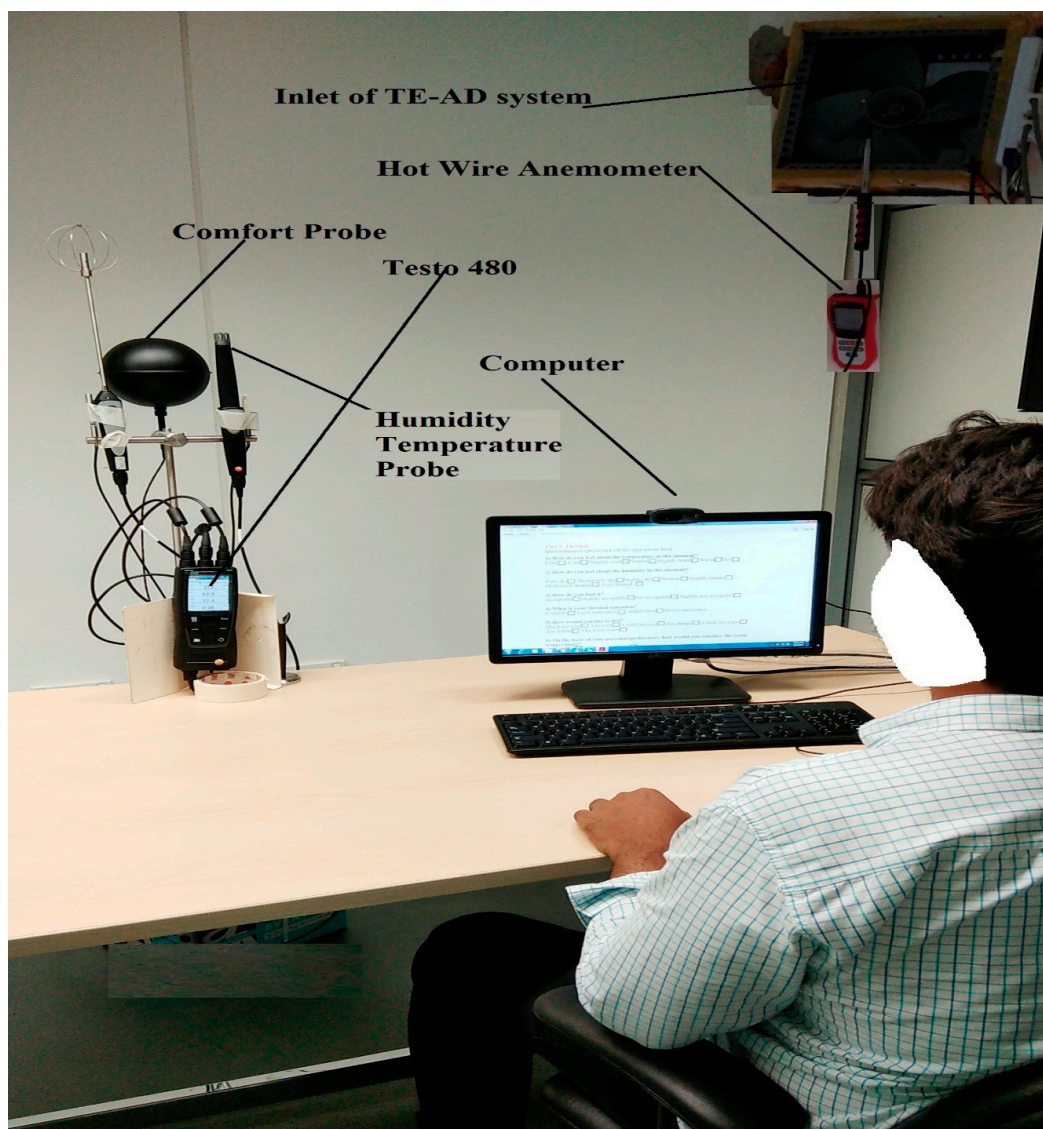


Figure 1. A study occupant registering his subjective opinion before the start of sleep experiment.

2.3. Description of Occupants

Thermal sensation, comfort level, quality of sleep of the occupants were recorded before and after the sleep using a survey form and air flow rate was recorded before and after the sleep. After waking up, the subjects also provided their feedback on the quality of their sleep during the night, which was recorded on the basis of a proforma used in an earlier study. An ASHRAE point scale proforma was used to record the thermal comfort, thermal sensation and thermal preference of the occupants.

2.4. Sleep Assessment

2.4.1. Sleeping Quality

In this experiment the wearable Fitbit Alta HR wristband watch was worn by the occupants to record sleep state and sleep efficiency measures such as body movement, heart rate, sleep-stage, and sleep quality. Fitbit watches are wearable activity trackers which are user-friendly and non-prominent. They are able to function by virtue of three axis Micro-Electro-Mechanical Systems (MEMS) accelerators, through which they record body movement and physiological parameters. The subjects were required to wear the Fitbit Alta HR watch over their non-dominant hand. Recent studies have pointed to the validity of the use of Fitbit devices for sleep studies in persons not showing clinical features of any sleep disorder. As compared to polysomnography too, Fitbit devices have demonstrated comparable efficiency in detecting state of sleep or wakefulness as also measuring sleep composition. REM sleep too can be estimated in a reliable manner by Fitbit devices [30]. Fitbit devices have been compared with Actigraphy and Fitbit devices have been found to be appropriate for sleep evaluations [31]. It was ensured that the subjects did not wear the device too tightly as it could impede blood flow and affect the heart signals. The signals received depend on the magnitude of body movement. The data were projected on a laptop and recorded using a wireless Bluetooth technology. Analysis of this data indicated the quality of sleep was derived in terms of the indices such as total sleep time (TST), sleep onset latency (SOL), heart rate (HR), sleep efficiency (SE), waking after sleep onset (WASO), and waking bouts (WB).

2.4.2. Thermal Environment During Sleeping

A wireless weather station (DAV005) was placed at a chosen spot on the test room. This measured outdoor macroclimatic conditions viz. temperature, relative humidity, solar irradiation, and speed and direction of the wind. The conditions inside the test room were measured and recorded by placing K-type thermocouples and hygrometers at selected spots. The indoor temperature and relative humidity were automatically recorded at intervals of 1 min in the multichannel data logger (Graptec GRA002 multichannel data logger, Japan). TESTO 480 probes were placed around the mid-point of the bed to record air velocity, dry and wet bulb globe temperatures, mean radiant temperature, air quality, as well as objective PMV and PPD. Subjective PMV and PPD is calculated by using Fanger's equation which was developed by analyzing filled questionnaire detail mentioned in Reference [19], given to each occupants during all sleep session.

As shown in Equation (1), $T_{comfort}$ (Temperature of comfort) is a function of T_{RM} (Mean running temperature) and T_{opt} (Operative temperature). Further, in order to calculate operative temperature (T_{opt}), radiant mean temperature (T_{mrt}) and heat transfer coefficient by convection (h_c) and radiation (h_r) were calculated as shown in Equation (1).

$$T_{opt} = \frac{h_c \times T_a \times h_r \times T_{mrt}}{h_c + h_r} \quad (1)$$

According to ASHRAE Standard 55 [22], T_{mrt} is determined by Equation (2).

$$T_{mrt} = \left[(T_g + 273)^4 + \frac{1.1 \times 10^8 V_a^{0.6}}{\varepsilon D^{0.4}} \times (T_g - T_a) \right]^{\frac{1}{4}} - 273 \quad (2)$$

where, the D is globe diameter and ε is the globe sensor surface temperature emissivity

Further according to the European Committee for Standardization (CEN standard) [32], T_{rm} is calculated by using Equation (3),

$$T_{rm(today)} = \alpha T_{rm(yesterday)} + (1 - \alpha) T_{m(today)} \quad (3)$$

where, $T_{rm(yesterday)}$ and $T_{rm(today)}$ are the mean running temperature for yesterday and today in °C, respectively. The $T_{m(today)}$ is the daily mean outdoor temperature of the day in °C, and an α of 0.8 was considered [33].

2.5. Adaptive Model

The adaptive comfort model of the test room used in this study is determined by linear regression. Using Griffiths method, the dependent variable $T_{comfort}$ and an independent variable T can be calculated by using Equation (4).

$$T_{comfort} = T + \frac{(0 - TSV)}{\alpha} \quad (4)$$

$T_{comfort}$ is the temperature of optimum comfort in °C, the T signifies the air temperature indoor, globe temperature or operative temperature, in °C. The thermal sensation vote before and after sleep is represented by TSV and "0" signifies condition of neutrality. The Griffiths coefficient α represents rate of change of TSV with air temperature of indoor climate. According to Humphreys et al. [34], α is set at values of 0.25, 0.33 and 0.5.

2.6. Data Analysis

The recorded data was log transformed and analyzed. Two samples t-tests were performed on the following variables- climatic conditions, sleep quality parameters, and subjective sensations, and variations in the data at different input values were predicted. The formula to calculate one sample t-test is given below in Equation (5).

$$t = \frac{\bar{x} - \mu}{s/\sqrt{n}} \quad (5)$$

All sleep quality parameters were examined using one-way Analysis of variance (ANOVA) test for repeated measures. Level of significance was set at 5% for both statistical tests. Please refer to the results section for details.

2.7. Experimental Procedure

The test chamber, described in Section 2.1 and the schematic diagram shown in Figure 2, has a cooling load of 589 W. In order to provide enough cooling TEMs each having 25 W cooling capacity were arranged inside the duct, details of which have been mentioned in previous studies [25,27]. The uncertainty analysis of measured parameters is also detailed in a previous study [27]. Twenty four TEMs were arranged inside the duct having cumulative cooling power of 600 W. The constant DC power supplier was used to provide six different incremental input current, i.e., (2 A, 3 A, 4 A, 5 A, 6 A and 7 A) at a fixed input voltage of 5 V, which in terms of operating power for twenty four (24) TEMs (240 W, 360 W, 480 W, 600 W, 720 W, and 840 W) were used to alter the microclimate of the test-room. The experimental conditions were arranged in such a manner that the TE-AD system was run at 240 W on the first night followed by the other operating powers on subsequent nights. Normalization of the test chamber was initiated 2 h preceding the start of the sleep study by powering on the TE-AD framework and the roof fan. Before the start of the trial, subjects were instructed to rest in the test-rooms for two consecutive nights as an adjustment period. The subjects were again briefed about the whole experiment. Anthropometric measurements such as weight, height, and body-to-mass-index of the subjects were taken in the preparation room one hour before the start of the sleep experiment (Figure 2). Regular recordings of room temperature, relative humidity and air flow

velocity as well as skin temperature, and heart rate of the subjects were taken. Subjects then sat on the bed in a relaxed manner to adapt to the test room surroundings. Fitbit Alta HR device in the form of a watch was worn by the occupants in sitting position. Before setting off to sleep, subjects were asked to complete a proforma pertaining to the indoor microclimate of the test chamber. The subjects were advised to recline for sleep at approximately 22:55, when the main lights were put off. The subjects covered themselves with a thin cotton sheet during sleeping as detailed earlier. Before they nodded off, the occupants were required to fill the thermal comfort survey form and then they were supposed to sleep from 23:15 to 07:00.

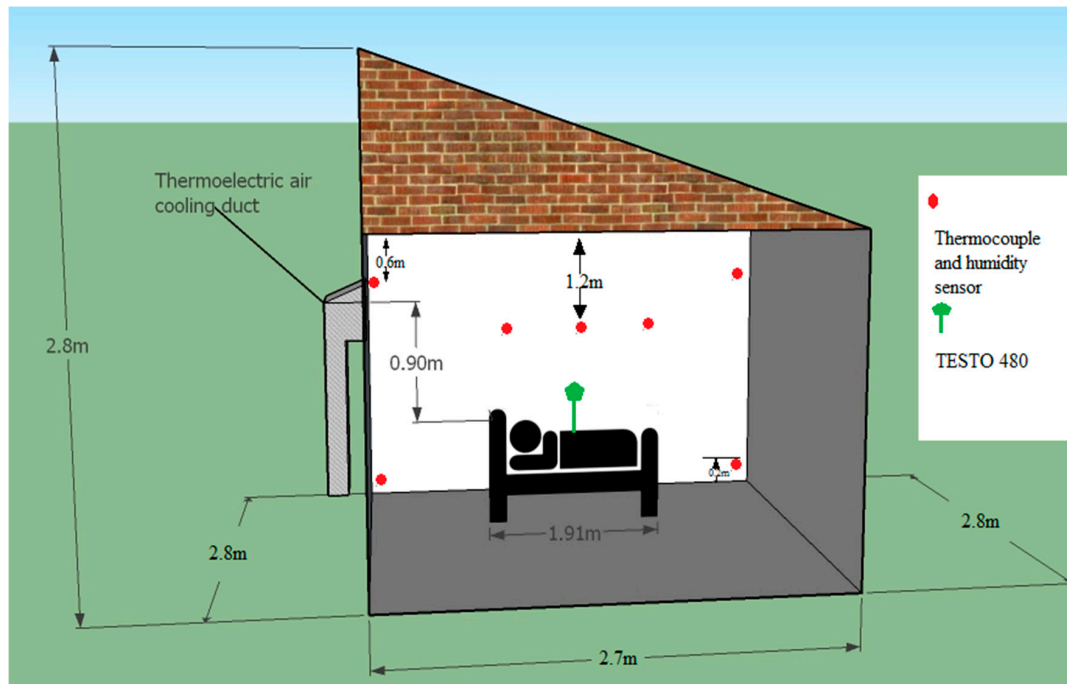


Figure 2. Schematic diagram of the test room used for sleeping analysis.

3. Results

3.1. Effect on Indoor Climatic Conditions

Experimental data were recorded at varying operating powers to the thermoelectric cooling system starting with 240 W up to 840 W, as described in the methodology. Variations in outdoors, indoors, center-of-bed temperature, as also relative humidity were recorded (Figures 3–6). Variations in the air flow velocity inside the test room are shown in Figure 7. Data obtained at 240 W were ignored as they did not provide significant changes in the indoor climatic conditions. To assess the difference between the mean scores of indoor temperatures obtained at operating power of 360 W and 480 W, a two-sample t-test was performed. The test statistics show a significant difference in the indoor temperature between 360 W and 480 W operating powers at 95% of confidence interval ($t = 6$, $df = 111$). The mean decrease in the indoor temperature from 480 W to 600 W was 0.389 °C, as shown in Figure 3. Indoor temperature data at operating power levels of 480 W was analyzed similarly, resulting in test statistics of ($t = 1.28$, $df = 111$), and a mean decrease in indoor temperature of 0.69 °C. Further increments in the operating power to TE-AD system, i.e., from 600 W to 720 W, significantly reduced the indoor temperature to ($M = 24.27 \pm 1.14$ °C). A comparison of temperatures at these two power levels from two-sample t-tests indicated ($t = 2.26$, $df = 111$) a mean decrease in the indoor temperature from 600 W to 720 W of 0.559 °C. Optimum performance in terms of temperature reduction was achieved at 720 W, and the mean indoor temperature achieved was ($M = 23.72 \pm 0.97$ °C). A comparison of temperatures obtained at 720 W and 840 W from two-tailed t-tests indicated

($t = -1.176$, $df = 111$) with a mean increase in the indoor temperature from 720 W to 840 W of 1.98 °C. ANOVA test was employed to estimate the difference between indoor temperatures at variable input currents and results show a significant change in the indoor temperature of the test chamber at variable power supplies with p value 0.000146 and F calculated value of 4.11.

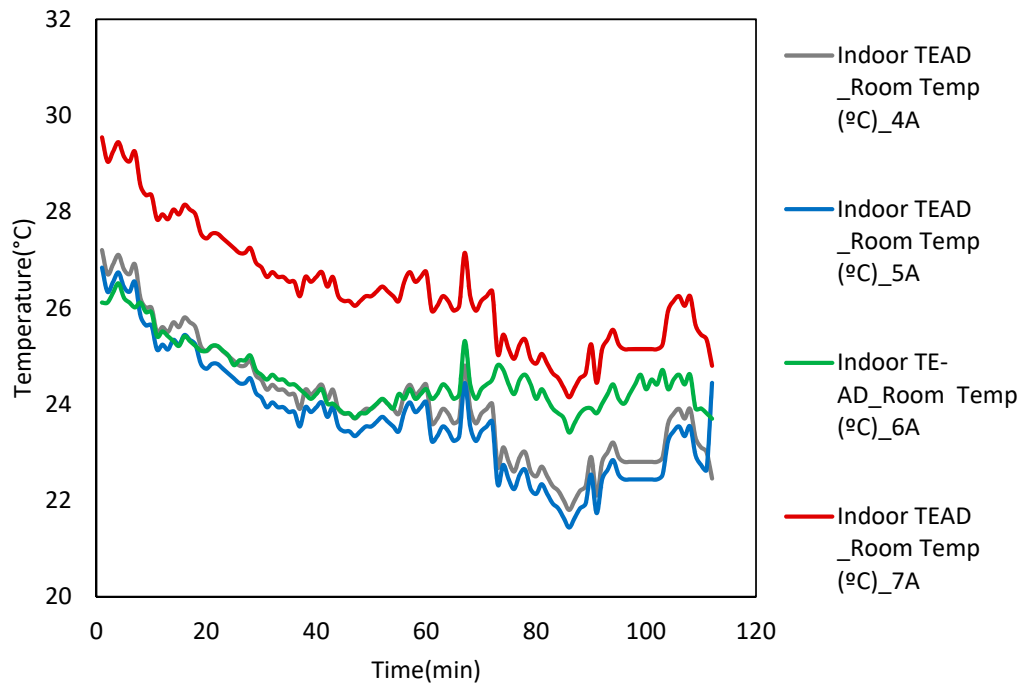


Figure 3. Changes in indoor and outdoor temperatures at different study power inputs.

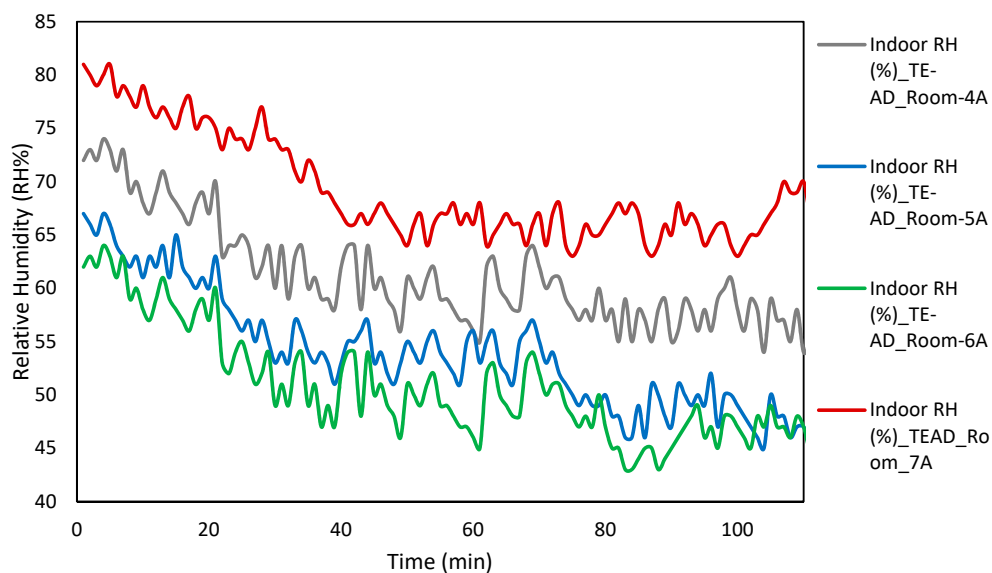


Figure 4. Changes in indoor and outdoor relative humidity at different study power inputs.

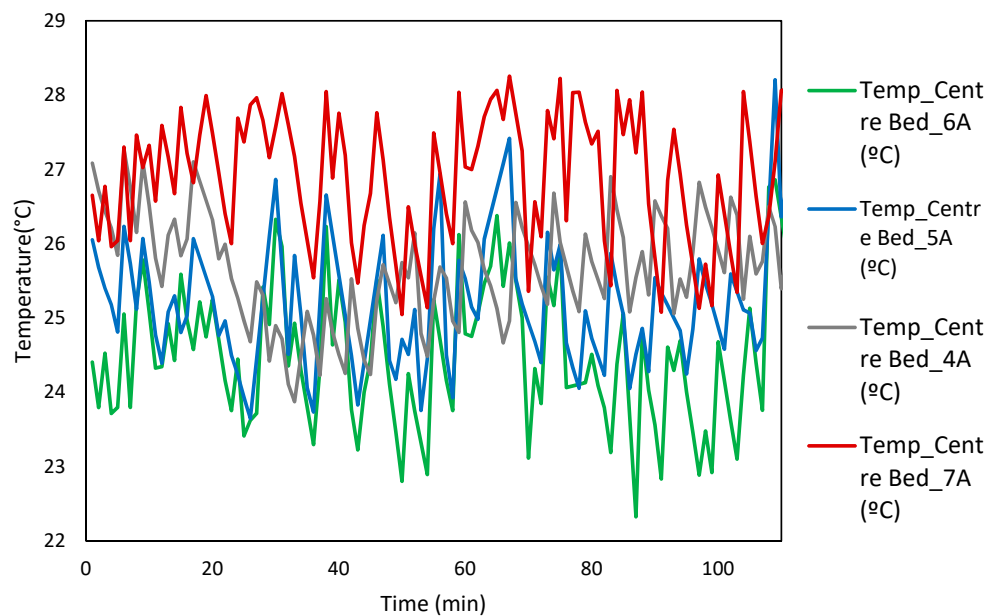


Figure 5. Variation of temperature at the center of the bed different power inputs.

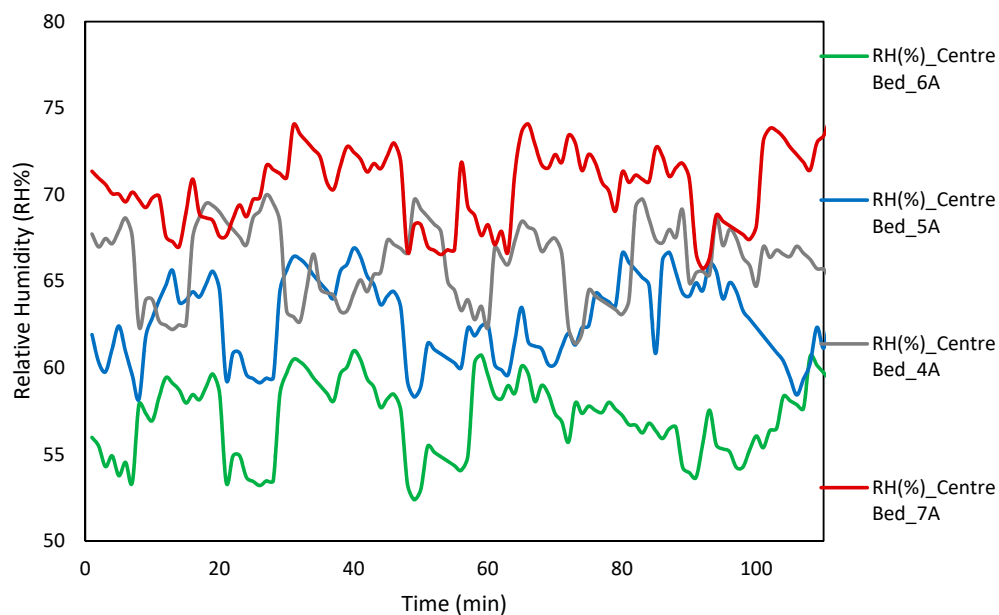


Figure 6. Variation of relative humidity near the mid-point of the bed at different operating powers.

Data pertaining to the mean scores of indoor relative humidity at input currents of 360 W and 480 W, were analyzed using a two-sample t-test. The indoor relative humidity showed a statistically significant decrease at operating power levels of 360 W ($M = 67.41 \pm 4.23$) as compared to operating power levels of 480 W ($M = 61.19 \pm 4.93$), with ($t = -5.732, df = 111$). A mean decrease of 6.23% in relative humidity was noted with a 95% confidence interval (Figure 4). By increasing the input current, a further decrement in the relative humidity inside the test room was observed ($M = 56.33 \pm 5.02$). The optimum relative humidity reduction was recorded when the TE-AD apparatus functioned at 720 W ($M = 51.43 \pm 4.93$) as compared to 600 W ($t = 24.45, df = 111$). Relative humidity inside the test room showed a mean decrease of 4.92% (95% CI) (Figure 4). A further increase in operating power to the TE-AD system to 840 W increased the percentage of relative humidity by 9.32%, which had a negative impact on the sleep comfort.

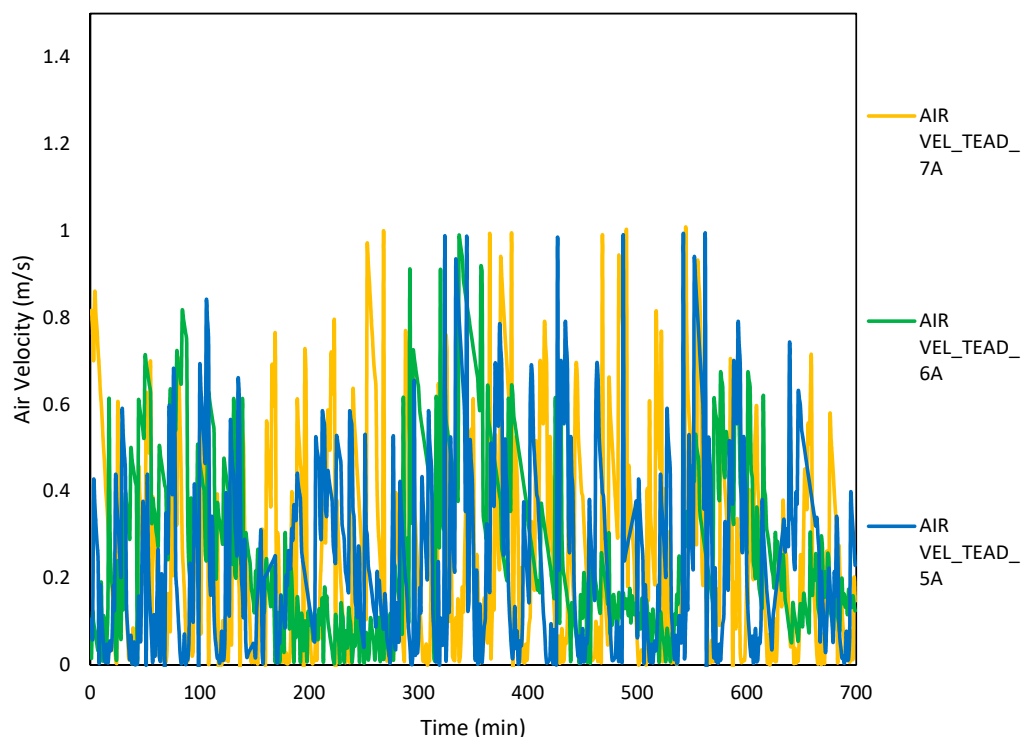


Figure 7. Variation of air velocity at different operating powers.

Variations in temperature and relative humidity near the mid-point of the bed are shown in Figures 5 and 6. In order to reduce redundancy in the graph, the variation of 480 W to 840 W is shown in Figures 5 and 6. To see the statistically significant variations of temperature and relative humidity at operating power of 360 W and 480 W, a paired-sample t-test was utilized. The decrease in temperature and relative humidity was statistically significant when compared between operating power levels of 360 W ($M = 26.22 \pm 0.75$ °C, $M = 68.21 \pm 2.31\%$) and 480 W ($M = 25.65 \pm 0.75$ °C, $M = 64.24 \pm 3.21$). The mean reduction in temperature and relative humidity were 0.57 °C and 3.77%, as shown in Figures 5 and 6. By raising the TE-AD apparatus power input to 600 W, the mean temperature and relative humidity decreased to ($M = 25.23 \pm 0.82$ °C, $M = 60.31 \pm 1.53$).

A further increment in the operating power input to the TE-AD system to 720 W decreased the temperature and relative humidity recorded close to the center of the bed by ($M = 24.49 \pm 0.94$ °C, $M = 55.48 \pm 3.23$). The temperature and relative humidity showed a rise when the operating power to the TE-AD system was raised from 720 W to 840 W, and the mean value increased to ($M = 26.49 \pm 1.12$ °C, $M = 68.731 \pm 4.021$).

Changes in indoor air velocity at different operating power to the TE-AD apparatus are shown in Figure 7. There is a significant change at 360 W and 480 W with ($t = 3.6$, $df = 698$) and a standard deviation of 2.19 was obtained for this combination. However, there was no significant change when comparing 480 W and 600 W with ($t = -1.39$, $df = 698$), standard deviation = 0.20. Similarly, the t-test showed no significant changes between 600 W and 720 W, 720 W and 840 W, and 360 W and 840 W. The maximum air velocity of 0.999 m/s was obtained at 840 W of current, and the smallest air velocity of 0.0001 m/s was obtained for 360 W of operating power.

3.2. Mean Skin Temperature

Changes in mean skin temperature (MST) of the subjects with the TE-AD operating under varying power conditions is shown in Figure 8. The average MST increased rapidly during the initial segment of the sleep. The average temperature remained at 34.7 °C for different operating powers 360 W to 840 W. A two-tailed t-test reported a significant change in the MST for each observation obtained

at different input currents. First, the test was conducted between 360 W and 480 W, with the t-stat ($t = 2.39$, $df = 144$) and a standard deviation of 0.2095 was found. Similarly, tests were conducted at operating power input power 360 W to 840 W, and all analyses showed significant changes for each data set as compared to those of other input currents. The mean skin temperatures at operating power from 360 W to 840 W were 35, 34.5, 34.6, 34.4, and 35.1 °C respectively.

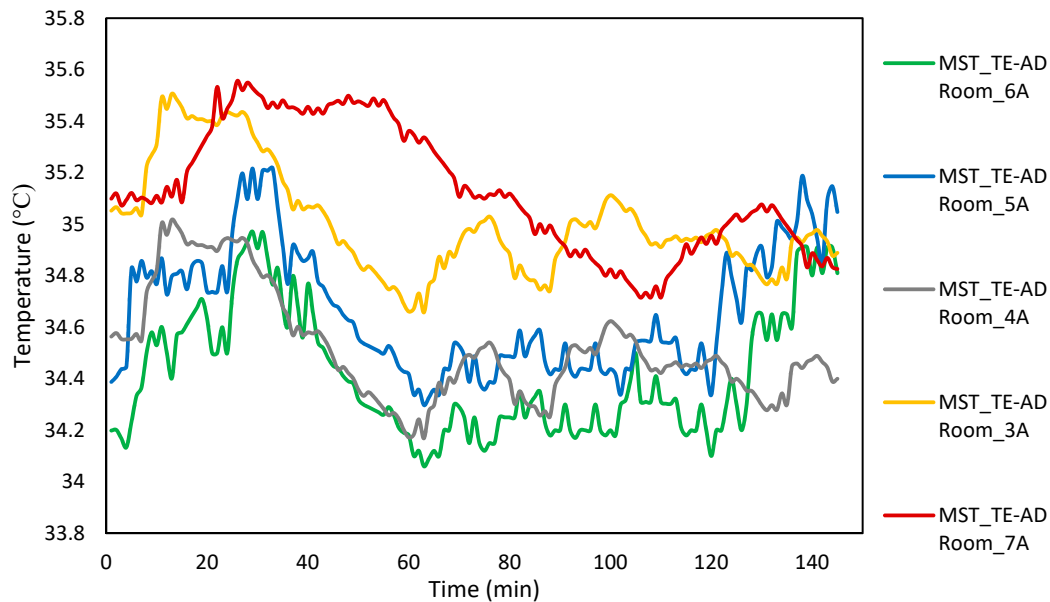


Figure 8. Variation in mean skin temperature at different operating powers.

3.3. Effects on Carbon Dioxide Generation

The variations in CO₂ generated inside the test room at different operating powers to the TE-AD apparatus are shown in Figure 9. A paired-sample t-test was utilized to assess the difference in the mean scores of CO₂ generation at operating power 360 W and 480 W and values of ($t = -3.5$, $df = 144$) at a 95% level of significance were obtained. This shows that the CO₂ increases with an increase in the input current. There was an increase in the indoor CO₂ content at an operating power of 480 W ($M = 621.52$) as compared to an operating power of 600 W ($M = 654.32$) which was found to be statistically significant. The t-test statistics was found as ($t = 2.64$, $df = 144$). The cooling effect produced by the TE-AD system increased by raising the operating power to the TE-AD system from 600 W to 720 W ($M = 673.42$), and the concentration of CO₂ increased to ($M = 713.43$). Further increments in the operating power to the TE-AD system to 840 W significantly reduced the CO₂ content inside the room to ($M = 621.64$). The TE-AD framework has turned out to be a standout among the most reliable and naturally well-disposed sustainable power source advancements, which assume a critical job in carbon dioxide emission mitigation. Analysis was performed to calculate the measure of CO₂ discharge moderated because of the current TE-AD framework when contrasted with ordinary cooling frameworks. The thermal power plant in Malaysia powered by coal discharges an average of 1.21 kg/kWh CO₂ [35]. Therefore, total CO₂ mitigation from existing TE-AD system was calculated for 1 year and compared with normal air-conditioning system by using Equation (6) as follows [36]:

$$\text{CO}_2 \text{ (kg/life)} = 1.21(\text{kg/kWh}) \times E \text{ (kWh/year)} \times n \text{ (year)} \quad (6)$$

The CO₂ emission of the TE-AD framework was recorded at operating power of 720 W and for air-conditioning system, 24 °C was taken as the reference temperature. The room-temperature set point for practically all the workplaces in Malaysia is in the 24–26 °C range. Further, it was assumed that both the systems, i.e., the TE-AD system and normal air conditioning system run for 8 h per night.

The total CO₂ emissions due to the TE-AD system for 1 year of operation was estimated to be 2.28 tons, as compared to 3.7 tons for the conventional air-conditioning system, a reduction of 1.4 tons (38%).

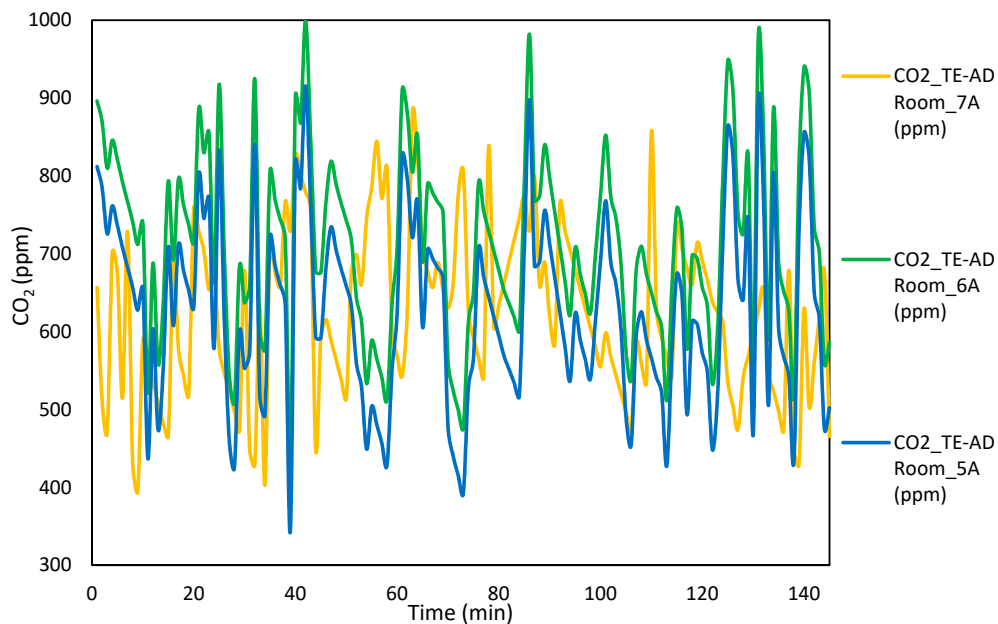


Figure 9. Variation of CO₂ at different power inputs.

3.4. Effect on Heart Rate

The heart rate of all occupants was recorded and analyzed under different input power situations. The results are shown in Figure 10. The maximum mean heart rate of 88.44 was observed at 360 W operating power, and the minimum mean heart rate (42.66 beats per minute) was registered at 720 W of power. An ANOVA test was carried out on heart rate data obtained under different TE-AD input power situations. The calculated values were as follows: F was 1.81 with 111 degrees of freedom (p value = 0.0013). The test showed there was a significant effect on the heart rates when the input power changed from 360 W to 480 W as well as when the input power was changed from 720 W to 840 W.

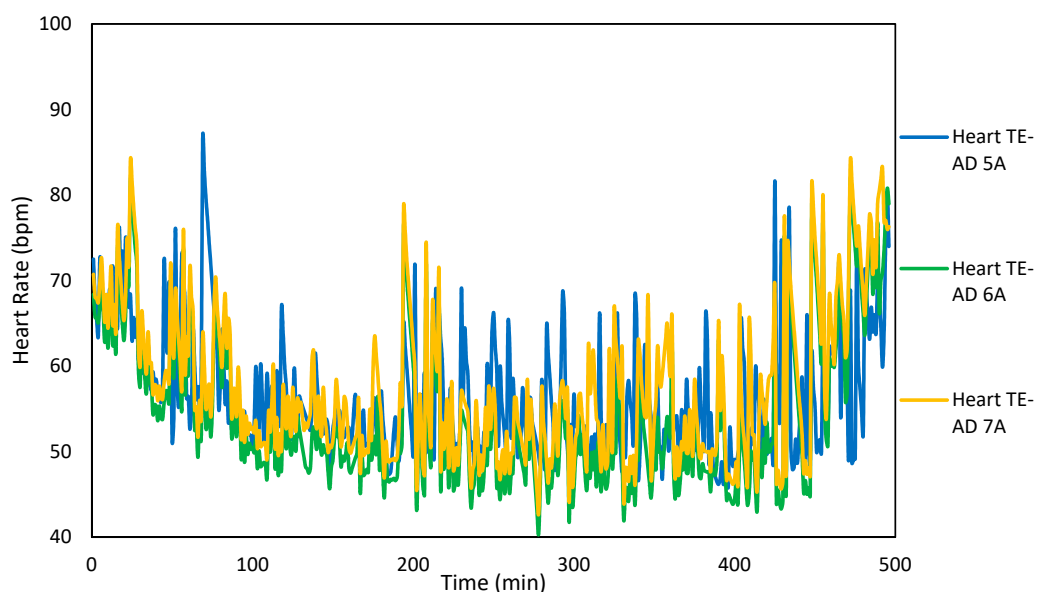


Figure 10. Variation in heart rate of the occupants at different operating powers.

3.5. Effect on Sleep Comfort Rating

The variations in the instrumental Predicted Mean Vote (PMV) and Predicted Percentage of Dissatisfied (PPD) ratings at different operating powers supplied to the TE-AD apparatus are shown in Figures 11 and 12. For analysis of variations in PMV and PPD at operating power of 360 W and 480 W, a two-sample t-test was conducted. A significant shift in the PMV and PPD ratings at operating power of 360 W (1.23 ± 0.42 , $M = 24.31 \pm 4.87$) to operating power of 480 W ($M = 0.84 \pm 0.32$, $M = 19.46 \pm 3.82$) was observed. The t-test values ($t = 27.1$, $df = 111$) and a 95% confidence interval. The mean shifts in the PMV and PPD ratings were 0.39 and 4.85% with a 95% confidence interval, as shown in Figures 11 and 12. An increment in the operating power to the TE-AD apparatus to 600 W shifted the PMV rating toward a neutral rating ($M = 0.45 \pm 0.48$) and decreased the percentage of dissatisfied occupants to ($M = 15.67 \pm 5.34$).

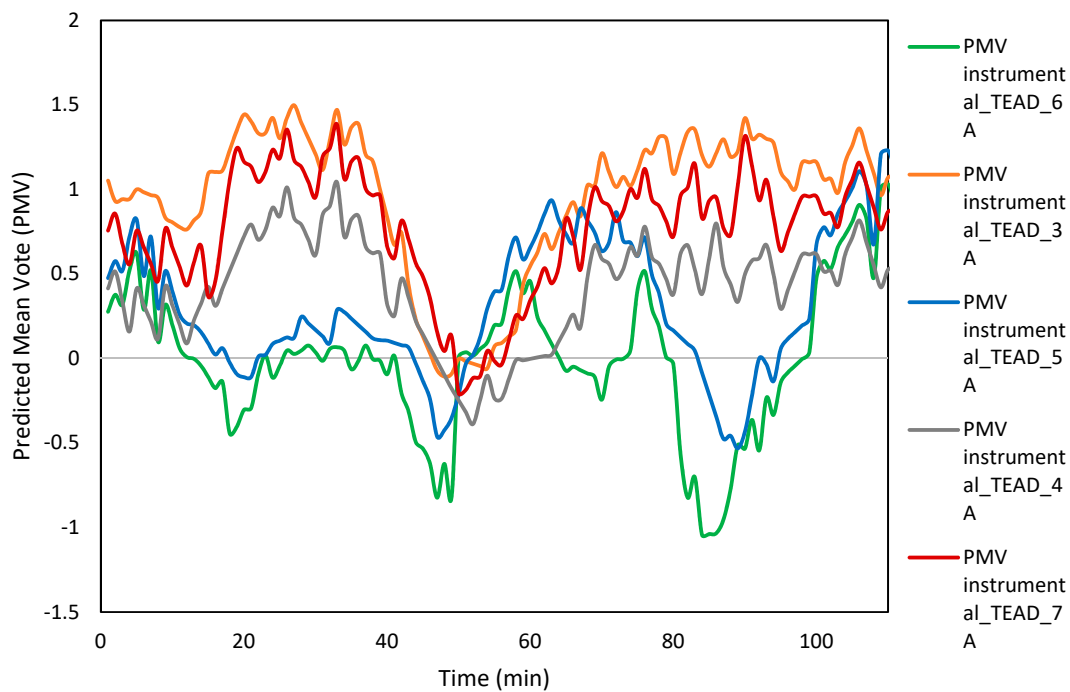


Figure 11. Variation in Predicted Mean Vote (PMV) at different operating powers.

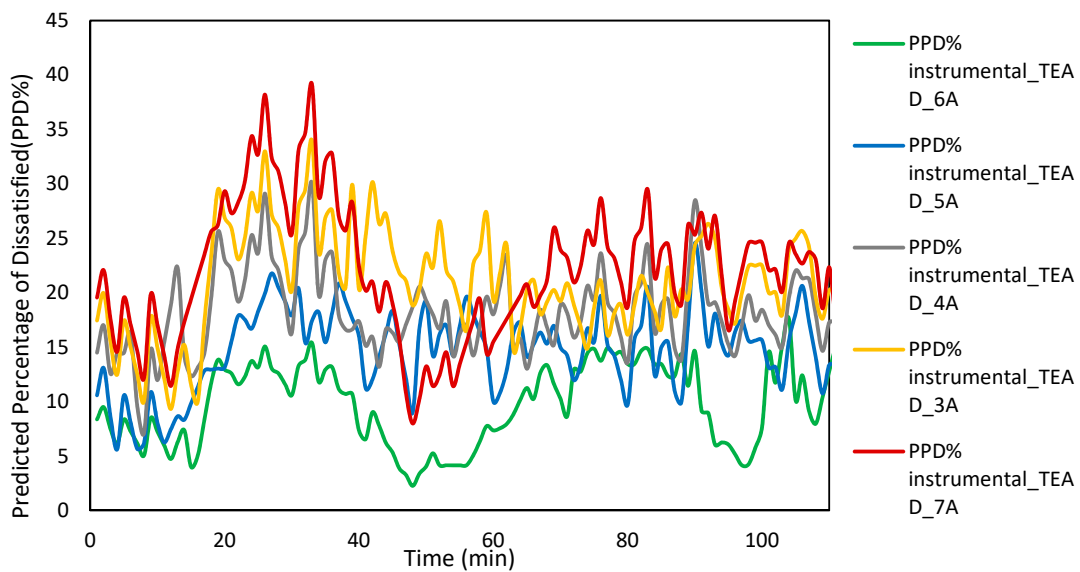


Figure 12. Variation of Predicted Percentage Dissatisfied (PPD %) at different operating powers.

Further improvements in the ratings were seen when the power input to the TE-AD system was raised to 720 W. Both the PMV ($M = -0.012 \pm 0.31$) and PPD ($M = 9.47 \pm 4.42$) ratings suggested that occupants felt more comfortable with their sleeping environment at 720 W power supply level. Deterioration in both the PMV ($M = 0.81 \pm 0.43$) and PPD ($M = 21.52 \pm 5.31$) ratings were observed when the operating power increased to 840 W.

3.6. Effect on Sleep Onset Latency, Sleeping Stage, and Comfort Sensation

Sleep onset latency variations at different operating power to the TE-AD system are shown in Figure 13. Comparison of data obtained at an input current of 360 W and 480 W by employing a paired-sample t-test shows significant variations in sleep onset latency (the $t = 3.56$). The mean sleep onset latency (SOL) time decreased from ($M = 40.7 \pm 0.98$ min) to ($M = 32.2 \pm 1.02$ min) by raising the operating power from 360 W to 480 W. The sleep onset latency time further decreased to ($M = 26.45 \pm 1.12$ min) when the TE-AD system was functioned at 600 W. A maximum reduction in sleep onset latency was recorded when the system was functioned at 720 W, and the mean time decreased to ($M = 18.33 \pm 1.18$ min). A further increment in the operating power input to the TE-AD apparatus increased the sleep onset latency time to ($M = 29.52 \pm 1.35$ min).

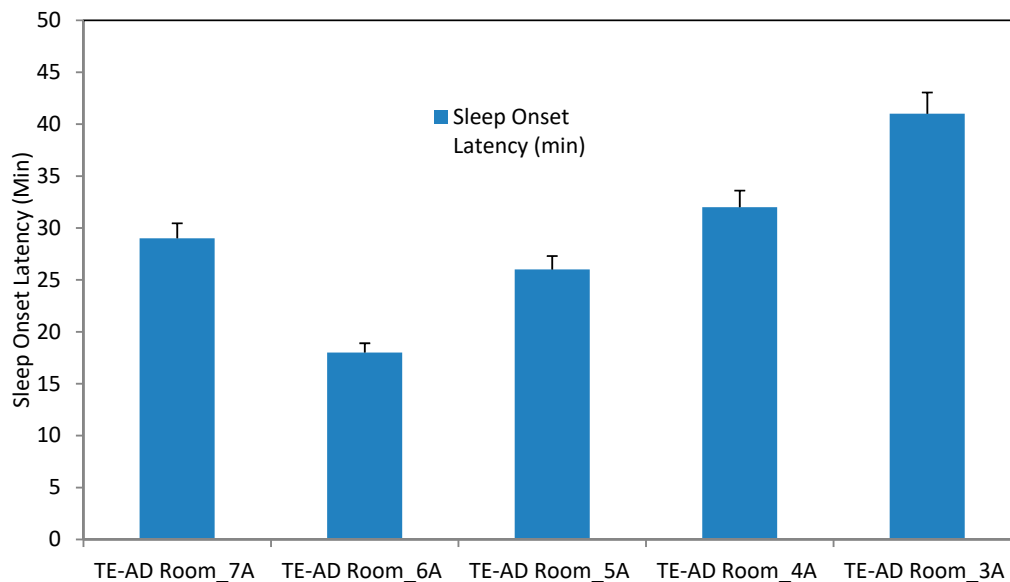


Figure 13. Variation in sleep onset latency with varying operating powers.

Sleep-stage variation of the subjects in relation to varying operating power has been shown in Figure 14.

Variation in comfort rating of the occupants when the operating power to the TE-AD was increased is shown in Figure 15. The comfort sensation assessment of the occupants varied significantly at 360 W as compared to 480 W ($t = -1.19$, 95% CI) as detailed in Figure 15. By increasing operating power to 480 W and then to 600 W comfort rating before and during sleep does not vary significantly ($t = 1.26$). Significant variations were observed when occupants gave a rating after waking up. Occupants reported an optimum comfort rating when the TE-AD apparatus was operated at 720 W. Comfort ratings after and during sleep do not vary significantly ($t = 1.01$, 95% CI). Significant variation was observed when occupants gave a rating before the start of sleep ($t = -0.89$). Shifting in comfort rating was observed at 840 W input to the TE-AD system. Rating after and during sleep does not vary significantly ($t = 0.986$), but significant variation was observed when occupants gave a rating before the start of sleep ($t = 3.68$).

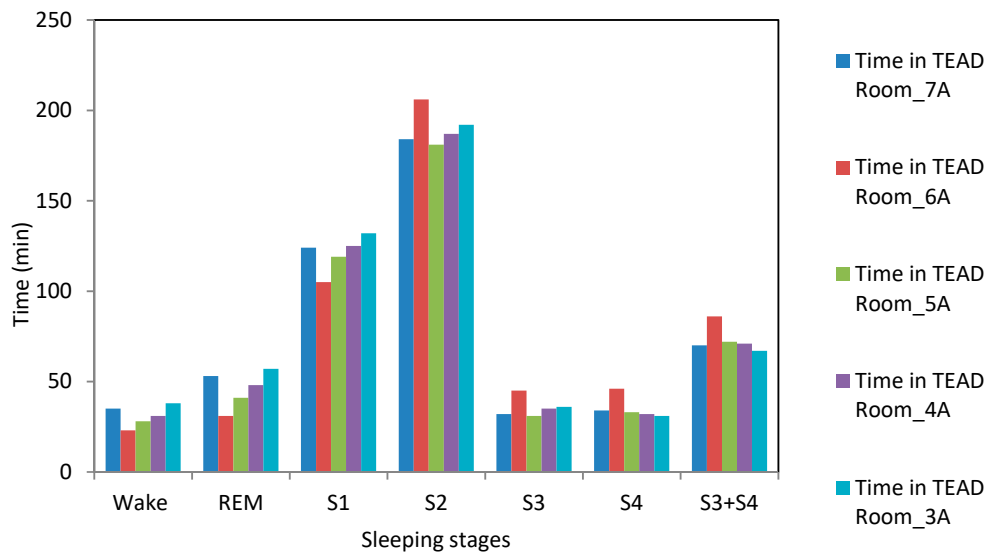


Figure 14. Variation in sleeping stage with varying operating powers.

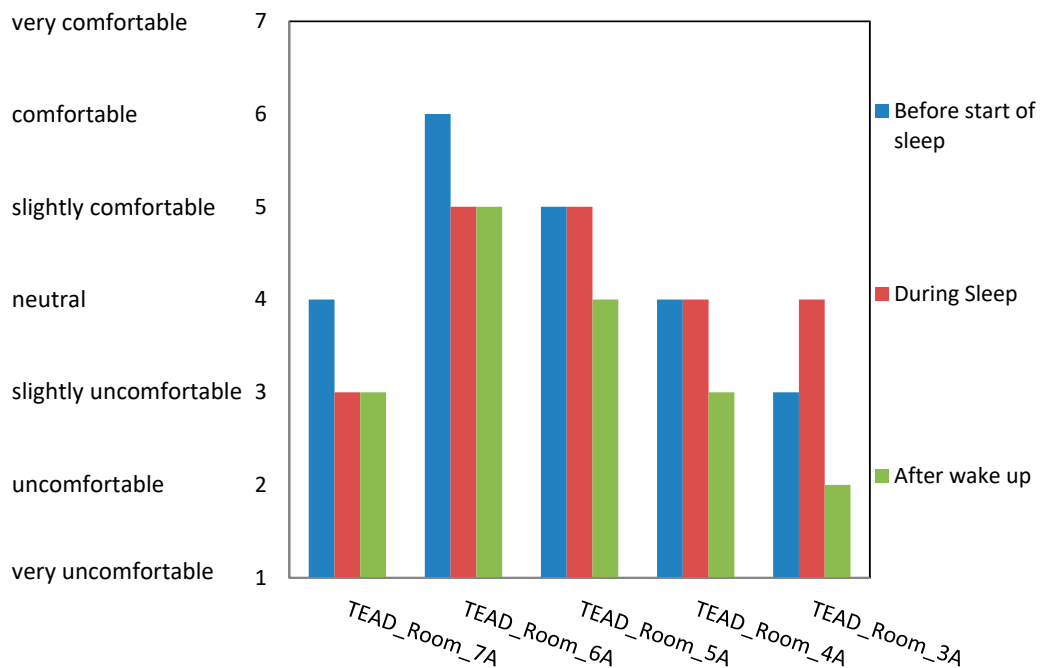


Figure 15. Variation in comfort sensation at different operating powers to the thermoelectric air duct (TE-AD) system.

Overall thermal comfort ratings of the occupants when the TE-AD is functioned at different power-inputs are presented in Figure 16. It was observed that overall thermal sensation ratings improve as operating power to the TE-AD is increased. At 360 W before and after sleep rating did not change significantly ($t = 1.21$), and significant variation was observed when the objective opinion was recorded during sleeping ($t = 2.98$). Overall thermal sensation ratings of occupants did not show significant variation before ($t = 1.85$) and during sleep ($t = 1.56$) when the TE-AD was functioned at 480 W and 600 W, but significant variation was observed when occupants gave a rating after waking up ($t = 4.56$). Optimum thermal sensation rating was observed at 720 W, where occupants sleep rating was not significantly different before ($t = 1.74$) and after sleeping ($t = 1.96$), while significant variation was observed when the objective readings recorded during sleeping was compared ($t = 2.36$). Occupants overall thermal sensation rating worsens as the operating power supply increases to 840 W.

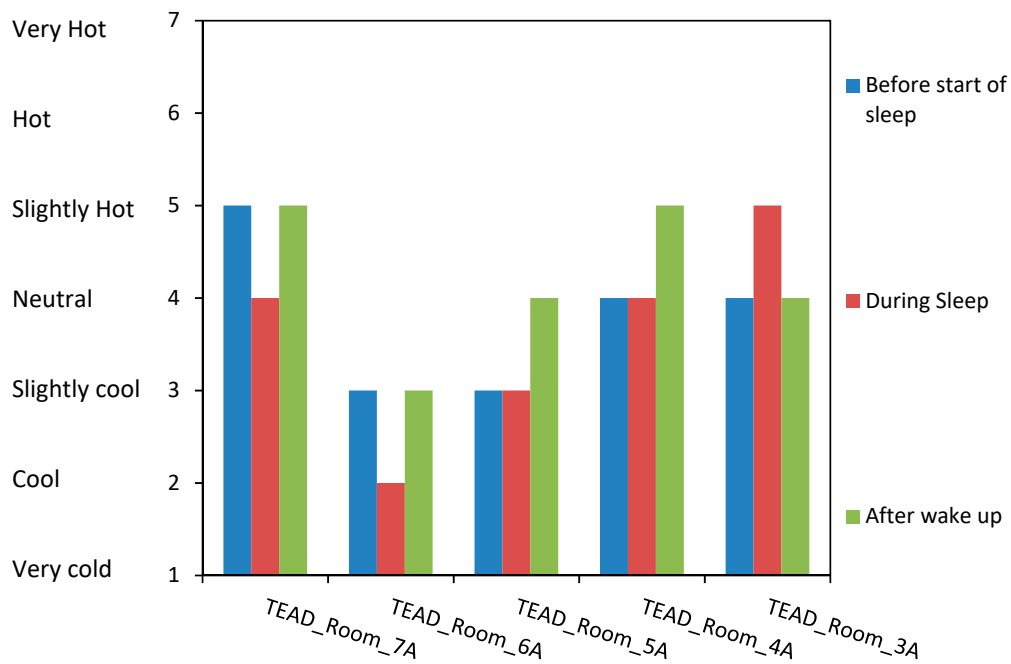


Figure 16. Variation in overall thermal sensation at different operating power.

3.7. Comfort Temperature

The comparison of the linear regression with the Pearson correlation in between variables T_a , T_g , T_{opt} is shown in Table 2. As per international standards [37,38] independent variable for the adaptive comfort model was chosen based on higher correlation coefficient and from Table 2 it is clear that $T_a:T_g$ is having smaller coefficient as compared to $T_a:T_{opt}$. Hence operative temperature is chosen as an independent variable.

Table 2. Regression and correlation between variables T_a , T_g , T_{opt} .

$T_a:T_{opt}$				$T_g:T_a$			
Equation	R ²	RMSE	<i>p</i>	Equation	R ²	RMSE	<i>p</i>
$T_{opt} = 0.876 \times T_a + 2.162$	0.9138	0.1835	<0.001	$T_g = 0.8289 \times T_a + 4.419$	0.9043	0.1731	<0.001

The Figures 17 and 18 show the regression lines and scatter plot of T_a , T_g and T_{opt} under the TE-AD cooling operation. It was found that the coefficient of correlation for $T_a:T_g$ is slightly lower than $T_a:T_{opt}$.

Furthermore, by using $T_{comfort}$ can be predicted by using the Griffiths method, using three Griffiths constant α (i.e., 0.25, 0.33, 0.50) as per researches performed by Humphreys et al. [34] and Mustapa et al. [39].

It was found from the above Table 3, the predicted comfort temperature is more stable when Griffiths constant $\alpha = 0.50$, where standard deviation is low.

Table 3. Prediction of comfort sleep temperature by the Griffiths method.

Condition	Sample Size (N)	Mean $T_{comfort}$ (SD)		
		$\alpha = 0.25$	$\alpha = 0.33$	$\alpha = 0.50$
TSV (4)	15	24.1(2.1)	24.1(1.9)	24.1(1.5)
TSV (1–3)	15	23.4(3.2)	22.8(3.8)	23.1(2.6)
TSV (5–7)	15	25.4(4.5)	26.2(3.7)	24.8(2.1)

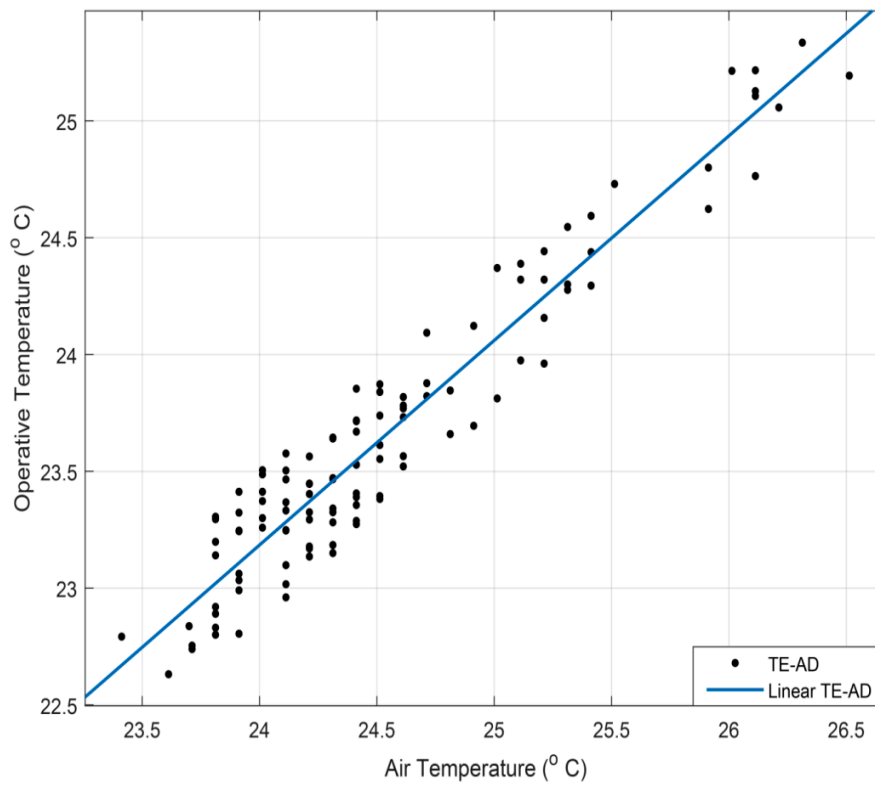


Figure 17. Linear regression between operative and air temperature.

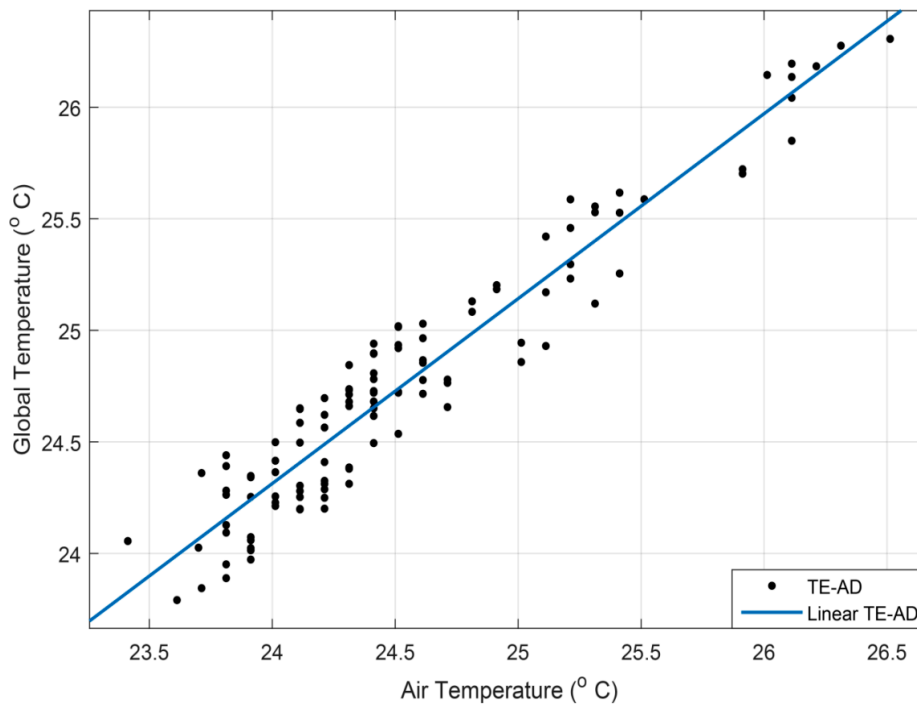


Figure 18. Linear regression between global and air temperatures.

3.8. Adaptive Thermal Comfort Model

The adaptive comfort model of test room with the TE-AD system can be obtained from the scatter plot as shown in Figure 19 having the linear regression between running mean temperature and comfort temperature.

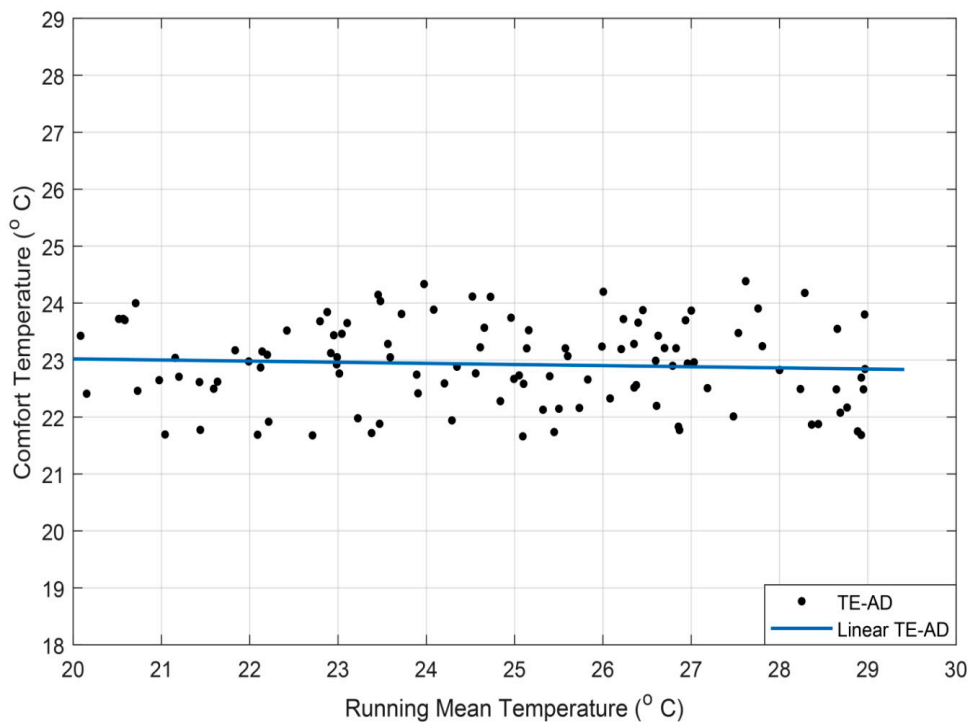


Figure 19. Adaptive comfort model of test chamber equipped with the TE-AD system and operated at 720 W.

The equation obtained from linear regression analysis represents the adaptive comfort model of test chamber with the TE-AD system as,

$$T_{comfort} = 0.3196 \times T_{rm} + 18.15 \quad (N = 15, R^2 = 0.987, p < 0.001) \quad (7)$$

This comfort temperature is directly dependent on mean running temperature of the test room as shown in Equation (7) and thus changes as the outdoor climatic condition changes. These changes can cause variation in the metabolic activity of occupants. The indoor conditions of the test room were adjusted by varying input power supply to the TE-AD system so that occupants can adopt the thermal condition of test room. This can be further explained by taking optimum condition of the TE-AD apparatus when running at input power of 720 W, the mean predicted $T_{comfort}$ was 23.7 ± 0.8 °C, with maximum and minimum values of 24.8 °C and 21.7 °C, respectively. These temperatures fall under the acceptability limit of adaptive comfort model which suggested that [40]

$$80\% \text{ acceptability higher limits} = T_c + 3.5 \text{ °C} \quad (8)$$

$$80\% \text{ acceptability lower limits} = T_c - 3.5 \text{ °C} \quad (9)$$

where 80% means that for acceptable condition of indoor comfort 80% occupants should comply with the $T_{comfort}$.

4. Discussion

Sleep has been identified to happen in distinct stages: stage of rapid eye movement (REM) sleep and stage of NREM sleep. There are 4 stages of NREM sleep, Stages 1 to 4, denoting an increasing depth of sleep from Stage 1 through Stage 4. Slow-wave sleep (SWS) is Stages 3 and 4 of the NREM. This is essential for the physical restoration of the person and is a useful parameter in sleep assessment [41]. SWS happens in the initial one-third of the night [42]. In contrast, the REM sleep is more in the last third part of a full night sleep. Sleep starts in NREM and progresses through the deeper stages of

sleep (Stage 1 to Stage 4) followed by REM sleep. The sleep alternates between NREM and REM with an approximately 90-min cycle. A normal person may have 4 to 6 such episodes during a 6–7 h sleeping period. As the night progresses the NREM stages become fewer, while the duration of REM sleep episode increases. Both the REM and NREM sleep are marked by physiologic variations such as changes in brain activity, sympathetic nervous system activity, muscle tone as well as variations in body temperature, heart rate, cerebral blood flow, blood pressure (BP), etc. As compared to waking state heart rate, blood pressure and brain blood perfusion are decreased during NREM sleep, while during REM sleep these parameters show an increase [11]. Apart from SWS, sleep onset latency (SOL) is another important measure of sleep quality. SOL is the time taken from reclining with an intent to sleep to the initiation of sleep. Usually, shorter the SOL, better is the quality of sleep. SOL is one of the main parameters which is deranged in persons suffering from insomnia [43].

Thermal environment affects sleep in a significant way [13]. The preoptic-anterior-hypothalamus (POAH) is a part of the brain which is responsible for thermoregulation. This center also regulates sleep [44]. There are several physiological changes related to thermoregulation studied in relation to sleep in humans. Heat dissipation from the body immediately before sleep is correlated with sleep onset latency which is an important indicator of sleep quality [45]. A number of researches have been undertaken to measure the comfort level of occupants during waking as well as sleep states in different thermally adapted conditions, especially the modifications of microclimate using air-conditioners. Air-conditioners use high energy intensive mechanical equipment for providing comfortable conditions. Therefore, the TE-ADs are an emerging technology, the efficiency of which is being tested in improving the microclimate of indoor spaces. Further, economic and energy consumption comparison of the commercially available air-conditioner with the TE-AD system shows significant benefits of the latter [46]. These are energy-efficient and eco-friendly and have the potential for large-scale use. However, research evaluating sleep quality in a test-space equipped with a TE-AD heating/cooling system for sleep conditions is still in the initial stages [29].

This study investigates the effects on sleep quality and thermoregulation in test-room conditions when the TE-AD framework is operated at variable power inputs (i.e., from 240 W to 840 W) in a tropical climate setting. The cooling power of the system gradually increased leading to a decrease in indoor temperature as well as relative humidity (RH%), when operating power was increased from 240 W to 720 W. However, when the operating power was further increased to 840 W, the cooling performance of the TE-AD deteriorated and indoor temperature as well as relative humidity increased (Figures 4 and 5). When the power to the TE-AD was set at 840 W, it underwent reverse heat transfer i.e., the hot sides of the TEMs started transferring heating back to the cold sides of the TEMs. Hence, 720 W was found to be the optimum power input for the TE-AD device used in the experiment. At operating power of 360 W and 840 W, the microclimatic conditions near the bed were worse. It was observed that variations in the mean skin temperature (MST) were dependent on the microclimatic parameters inside the test chamber. Elevated temperature and RH% affects the physiology of humans [47]. Variations in the microclimatic heat-level leads to the generation of a sympathetic reflex [48] which causes changes in the skin temperature. Increase in peripheral blood flow is the physiological response of the body to any rise in microclimatic temperature which is intended to increase heat losses through the surface of the skin [49]. The dilated peripheral blood vessels increase the mean skin temperature, which is controlled by either of the two pathways—the noradrenergic system (blood vessel constriction) or the adrenergic system (blood vessel dilation). The mean RH% at 360 W and 840 W were higher, which created thermal stress in the occupants during sleep as a higher RH% is an impediment to thermoregulation. Sweat rate is highest in SWS. Hence, a decrease in sweat rate affects the SWS sleep. Additionally, as REM is most sensitive to the ambient temperature, the REM was also affected when the room temperature was high [50]. The occupants took additional time while changing from the waking state (WS) to REM when the TE-AD framework was worked at both 360 W and at 840 W. Additionally, the duration of deep-sleep was shorter, as was the length of the NREM, i.e., the sleep quality was poorer in these cases. Higher relative humidity and higher temperature in the early segment of the sleep affects the sleep

stages more than the later segments [50] and [51]. A high ambient temperature and RH% affects the overall sleep quality.

The sleep onset latency time was more when the TE-AD was functioned at 360 W and 840 W as compared to 600 W and 720 W, as shown in Figure 14. This increase in SOL is because of high temperature and RH% near the center of the bed, which causes a decrease in the total sleep duration and a reduction in SWS and REM durations, and increased wakefulness and sleep onset latency time, as also suggested by another researcher [52]. A little decrease in the test-room temperature and relative humidity by raising the operating power to the TE-AD caused a more favorable objective and subjective feedback of occupants as regards the sleep quality. This was also suggested by the authors of Reference [53] in their study of sleep quality under microclimate modified by using air-conditioners.

Both objective and subjective assessments of comfort level and overall thermal sensation at operating power levels of 360 W and 840 W suggested that tenants were not comfortable with the sleeping environment at these inputs, as shown in Figures 16 and 17. At 360 W power input to the TE-AD framework, tenants assessed the indoor climatic environment as uncomfortable to some extent (3) before the start of sleep, and changed their opinion after waking up to uncomfortable (2). However, the objective rating during sleep suggested a neutral (4) indoor condition. Occupants rated the overall thermal comfort sensation in the given indoor climatic conditions as slightly hot (5) during and after sleep, although at the start of the experiment, the occupants had rated the indoor microclimate as neutral (4), as shown in Figure 17. The PMV and PPD ratings, as shown in Figures 12 and 13, support the above results concluding that 24% of the subjects were not satisfied with the microclimatic conditions of the test chamber.

A further increment in the operating power to 480 W and then to 600 W improved the cooling effect of the TE-AD. When air passed through the cold sides of the TEMs, the temperature and moisture content got decreased. This cool, dehumidified air reduced the temperature and relative humidity inside the room. The microclimatic conditions adjacent to the center of the bed were improved and created a more conducive sleeping environment. The sleeping comfort level of the occupants and overall thermal sensation ratings were progressively improved as the TE-AD operation progressed from 480 W to 600 W. Occupants that were rating a neutral (4) comfort sensation before and during sleeping at a TE-AD operation of 480 W shifted their ratings to slightly comfortable (5) for indoor climatic conditions at 600 W. Meanwhile, the after-sleep rating at 480 W was slightly uncomfortable (3) but changed to neutral at 600 W operating power. The overall thermal sensation ratings also suggest that the opinions of the subjects before and during sleep were neutral (4) at 480 W, but changed to slightly cool (3) for the indoor thermal climate at 600 W. In addition, the after-sleep opinions, which were slightly hot (5) at 480 W, changed to neutral (4) at 600 W. The mean skin temperature (MST) was also reduced by raising the operating power to the TE-AD framework from 480 to 600 W. This decrease resulted from reduction in the temperature as well as RH% in the test room, facilitating better heat dissipation from the skin. The PMV and PPD ratings support the above results and suggest that the PPD percentage of occupants at 480 W was improved from 19.4% to 15.4% at 600 W. Therefore, more subjects were satisfied with the indoor microclimate of the test room during sleep, as shown in Figures 12 and 13.

The optimum cooling performance of the TE-AD system was achieved when it was operated at 720 W. The indoor temperature and relative humidity decreased to 23 °C and 51%, respectively. The core body temperature of the occupants (T_{core}) diminished during this stage owing to the circadian rhythm as well as progression of the sleep [54]. T_{core} decreases because of a loss of heat from the skin surface which occurs due to vasodilation of the arteriovenous anastomoses [55]. An increased MST normally occurs because of the reduced activity of noradrenergic blood vessel constricting tone, thus allowing more blood influx from the core at higher temperatures. This leads to loss of heat from the skin surface to the surroundings [56]. Tenants that were rating a comfortable (6) pre-sleep sensation at a TE-AD operation of 720 W shifted their ratings to slightly comfortable (5) for indoor climatic conditions during and after sleeping. At the operating power of 720 W, the overall thermal sensation ratings of the

occupants before sleep was slightly cool (3), which changed to cool (2) after sleep—an increase in cold perception. The mean skin temperature was also reduced when the operating power was increased to 720 W. This reduction resulted from a change of the microclimate of the room—decreased temperature as well as relative humidity, which facilitated better heat dissipation. The PMV and PPD ratings also support the above results and suggest that the PPD percentage of occupants improved to 9% at 720 W. Therefore, more tenants were pleased with the indoor sleeping conditions of the test chamber as shown in Figure 13, and the room met the ASHRAE 55 standards [57] criteria for comfortability.

Figure 11 shows heart-rate variation of the occupants under different stages of sleep when TE-AD system was operated under different operating power. It was found that the 360 W and 840 W operating power caused greater variation in heart rate as compared to other input powers. The heart and respiratory rates of the subjects declined with progression in sleep stages from attentiveness to REM so as to adjust to the slowdown in body metabolism. The mean heart rate also showed a decrease as the occupant entered S1 and after that to S3 + S4 (SWS). This reduction in the heart rate happened because the neuronal signals that raise the pulse rate of the subjects were inhibited, and the nerve signals that bring down the pulse rate were stimulated. Somer et al. [58] discovered that stages of sleep have an influence on the cardiovascular performance. During REM heart rate as well as respiratory activity is more as compared to wakefulness and NRE [58]. Occupants heart and respiratory rates were higher when the operating power to the system was 360 W as well as 840 W, due to hotter and more humid microclimatic conditions. This condition leads to shifting in sleep stage from NREM sleep to REM sleep. When the power input to the TE-AD framework was increased from 480 W to 720 W, the cooling capacity of the system also increased leading to better regulation of the sleep stages and improved overall sleep quality. This real scale study provide alternative air-cooling mechanism which is free from refrigerant, compressor, evaporator, condenser and pumps with high reliability and less maintenance. As TEMs required direct electrical current for its operation, future studies can focus on changing power source from grid to solar photovoltaic system.

5. Conclusions

This research analyzes the subjective and objectives parameters of sleep quality of volunteer-occupants who slept in a test chamber with a TE-AD framework operated at six pre-determined levels of input supply, i.e., 240 W to 840 W. The conclusions are:

- When the operating power to the TE-AD framework was raised from 240 W to 720 W, the cooling capacity of the framework increases, causing a decrease in room temperature as well as relative humidity.
- The sleep satisfaction level of the subjects was increased by raising the power input to the TE-AD framework. Shifts in sleeping stages and heart-rate variability were at a minimum when the TE-AD framework was functioned at 720 W. The 720 W input power supply provided optimum sleeping comfort as compared to other levels of the input power.
- Increasing the power supply beyond 720 W reduced the cooling function of the system drastically resulting in a lowering of the sleep quality and overall thermal sensation; increase in sleep onset latency time, increased sleep stages shifting frequency, increased heart rate, and a decrease in PMV and PPD ratings.
- Of the six operating powers, it was at 360 W as well as 840 W operation of TE-AD, that the SOL of the test-room occupants was greatest and it was at a minimum when it was functioned at 600 W and at 720 W. At 720 W of input power, the occupants spent lengthier time in the NREM sleeping stage in contrast to operating inputs of 360 W or 840 W.
- Both the PMV and PPD ratings revealed that most of the tenants were thermally satisfied with the test-chamber microclimate when the TE-AD framework was operated at 720 W. At this power input, the PMV rating was in the range of ± 0.5 , and PPD was in the range of 9%, thus meeting ASHRAE Standard 55.

- The adaptive comfort temperature predicted $T_{comfort}$ was 23.7 ± 0.8 °C, at maximum and minimum values of 24.8 and 21.7 °C, respectively.
- Optimizing power of operation of the TE-AD is environmentally sustainable. Estimated reduction in CO₂ emission was calculated to be around 38% as compared to the conventional air-conditioning.

Author Contributions: K.I. designed and performed the experiments, derived the models, drafted the manuscript and analysed the data. S.A. performed review and provide solution to reviewers comments. M.T.A. involved in planning and supervised the work, processed the experimental data, performed the analysis, and designed the figures. S.A.I. contributed to the design and implementation of the research, to the analysis of the results and to the writing of the manuscript. K.H. subject arrangement and analysis, prototype development and performing experimental task. M.A.H.A. arranging fund, contributed to the interpretation of the results, supervised the project. M.H.Z. provide solution to reviewers comments and critical reviewing manuscript. G.M.S.A. aided in interpreting the results and worked on the manuscript.

Funding: This research was funded by Deanship of Scientific Research at King Khalid University under grant number R.G.P1./95/40.

Acknowledgments: The authors extend their appreciation to the Deanship of Scientific Research at King Khalid University for funding this work through Research Group Project under grant number (R.G.P1./95/40). The experiments were performed at Universiti Teknologi PETRONAS (UTP), Malaysia for which the authors are indebted to the institution.

Conflicts of Interest: The authors declare no conflict of interest.

Nomenclature

\bar{x}	sample mean;
CO ₂	carbon dioxide;
COP	coefficient of performance;
CI	confidence interval;
D	globe diameter (m);
df	degree of freedom
E	energy (kWh/year)
h_c	heat transfer coefficient by convection, W/(m ² K);
h_r	heat transfer coefficient by radiation, W/(m ² K);
MST	mean skin temperature;
n	years;
N	number of participants;
n	sample size;
NREM	non-rapid eye movement;
p	significance level of the regression coefficient;
PMV	predictive mean vote;
PPD	predicted percentage dissatisfied;
PSQI	Pittsburgh sleep quality index;
R^2	coefficient of determination;
REM	rapid eye movement;
s	sample standard deviation;
SOL	sleep onset latency;
T_a	air temperature (°C);
$T_{comfort}$	temperature of comfort (°C);
TE-AD	thermoelectric air duct system;
TEM	thermoelectric module;
T_g	globe bulb temperature (°C);
$T_{m(today)}$	the daily mean outdoor temperature of the day (°C);
T_{mrt}	radiant mean temperature (°C);
T_{opt}	operative temperature (°C);
T_{RM}	mean running temperature (°C);
$T_{rm(today)}$	the mean running temperature for today (°C);
T_{mrt}	radiant mean temperature (°C);

TSV	thermal sensation vote;
v_a	velocity of air, m/s;
α	Griffiths constant;
ε	the globe sensor surface temperature emissivity;
μ	hypothesized population mean

References

1. He, M.; Lian, Z.; Chen, P. Evaluation on the performance of quilts based on young people's sleep quality and thermal comfort in winter. *Energy Build.* **2019**, *183*, 174–183. [[CrossRef](#)]
2. Lan, L.; Tsuzuki, K.; Liu, Y.F.; Lian, Z.W. Thermal environment and sleep quality: A review. *Energy Build.* **2017**, *149*, 101–113. [[CrossRef](#)]
3. Joshi, S.S.; Lesser, T.J.; Olsen, J.W.; O'Hara, B.F. The importance of temperature and thermoregulation for optimal human sleep. *Energy Build.* **2016**, *131*, 153–157. [[CrossRef](#)]
4. Zhu, M.L.; Ouyang, Q.; Shen, H.G.; Zhu, Y.X. Field study on the objective evaluation of sleep quality and sleeping thermal environment in summer. *Energy Build.* **2016**, *133*, 843–852. [[CrossRef](#)]
5. Lan, L.; Lian, Z.W.; Qian, X.L.; Dai, C.Z. The effects of programmed air temperature changes on sleep quality and energy saving in bedroom. *Energy Build.* **2016**, *129*, 207–214. [[CrossRef](#)]
6. Bruelisauer, M.; Chen, K.W.; Iyengar, R.; Leibundgut, H.; Li, C.; Li, M.; Mast, M.; Meggers, F.; Miller, C.; Rossi, D.; et al. BubbleZERO-design, construction and operation of a transportable research laboratory for low exergy building system evaluation in the tropics. *Energies* **2013**, *6*, 4551–4571. [[CrossRef](#)]
7. Widiatmojo, A.; Chokchai, S.; Takashima, I.; Uchida, Y.; Yasukawa, K.; Chotpantararat, S.; Charusiri, P. Ground-source heat pumps with horizontal heat exchangers for space cooling in the hot tropical climate of Thailand. *Energies* **2019**, *12*, 1274. [[CrossRef](#)]
8. Lim, J.; Yoon, M.S.; Al-Qahtani, T.; Nam, Y. Feasibility study on variable-speed air conditioner under hot climate based on real-scale experiment and energy simulation. *Energies* **2019**, *12*, 1489. [[CrossRef](#)]
9. Escandón, R.; Suárez, R.; Sendra, J.J.; Ascione, F.; Bianco, N.; Mauro, G.M. Predicting the impact of climate change on thermal comfort in a building category: The Case of Linear-type Social Housing Stock in Southern Spain. *Energies* **2019**, *12*, 2238. [[CrossRef](#)]
10. Pan, L.; Lian, Z.; Lan, L. Investigation of Gender Differences in Sleeping Comfort at Different Environmental Temperatures. *Indoor Built Environ.* **2012**, *21*, 811–820. [[CrossRef](#)]
11. Harding, K.; Feldman, M. Sleep Disorders and Sleep Deprivation: An Unmet Public Health Problem. *J. Am. Acad. Child Adolesc. Psychiatry* **2008**, *47*, 473–474. [[CrossRef](#)]
12. Olesen, J.; Gustavsson, A.; Svensson, M.; Wittchen, H.U.; Jönsson, B. The economic cost of brain disorders in Europe. *Eur. J. Neurol.* **2012**, *19*, 155–162. [[CrossRef](#)] [[PubMed](#)]
13. Okamoto-Mizuno, K.; Mizuno, K. Effects of thermal environment on sleep and circadian rhythm. *J. Physiol. Anthropol.* **2012**, *31*, 1–9. [[CrossRef](#)] [[PubMed](#)]
14. Morito, N.; Tsuzuki, K.; Mori, I.; Nishimiya, H. Effects of two kinds of air conditioner airflow on human sleep and thermoregulation. *Energy Build.* **2017**, *138*, 490–498. [[CrossRef](#)]
15. Yang, B.; Olofsson, T. A questionnaire survey on sleep environment conditioned by different cooling modes in multistorey residential buildings of Singapore. *Indoor Built Environ.* **2015**, *26*, 21–31. [[CrossRef](#)]
16. Pan, L.; Lian, Z.; Lan, L. Investigation of sleep quality under different temperatures based on subjective and physiological measurements. *HVAC R Res.* **2012**, *18*, 1030–1043.
17. Irshad, K.; Habib, K.; Saidur, R.; Kareem, M.W.; Saha, B.B. Study of thermoelectric and photovoltaic facade system for energy efficient building development: A review. *J. Clean. Prod.* **2019**, *209*, 1376–1395. [[CrossRef](#)]
18. Liu, D.; Cai, Y.; Zhao, F.Y. Optimal design of thermoelectric cooling system integrated heat pipes for electric devices. *Energy* **2017**, *128*, 403–413. [[CrossRef](#)]
19. Irshad, K.; Khan, A.I.; Algarni, S.; Habib, K.; Saha, B.B. Objective and subjective evaluation of a sleeping environment test chamber with a thermoelectric air cooling system. *Build. Environ.* **2018**, *141*, 155–165. [[CrossRef](#)]
20. Lertsatitthanakorn, C.; Wiset, L.; Atthajariyakul, S. Evaluation of the thermal comfort of a thermoelectric ceiling cooling panel (TE-CCP) system. *J. Electron. Mater.* **2009**, *38*, 1472–1477. [[CrossRef](#)]

21. Maneewan, S.; Tipsaenprom, W.; Lertsatitthanakorn, C. Thermal comfort study of a compact thermoelectric air conditioner. *J. Electron. Mater.* **2010**, *39*, 1659–1664. [[CrossRef](#)]
22. ASHRAE Handbook—HVAC Applications; ASHRAE: Atlanta, GA, USA, 2007. Available online: <https://app.knovel.com/web/toc.v/cid:kpASHRAE12/viewerType:toc/> (accessed on 27 May 2018).
23. Lertsatitthanakorn, C.; Tipsaenprom, T.; Srisuwan, W.; Atthajariyakul, S. Study on the cooling performance and thermal comfort of a thermoelectric ceiling cooling panel system. *Indoor Built Environ.* **2008**, *17*, 525–534. [[CrossRef](#)]
24. Irshad, K.; Habib, K.; Basrawi, F.; Thirumalaiswamy, N.; Saidur, R.; Saha, B.B. Thermal comfort study of a building equipped with thermoelectric air duct system for tropical climate. *Appl. Therm. Eng.* **2015**, *91*, 1141–1151. [[CrossRef](#)]
25. Irshad, K.; Habib, K.; Kareem, M.W.; Basrawi, F.; Saha, B.B. Evaluation of thermal comfort in a test room equipped with a photovoltaic assisted thermo-electric air duct cooling system. *Int. J. Hydrogen Energy* **2017**, *42*, 26956–26972. [[CrossRef](#)]
26. Kimmling, M.; Hoffmann, S. Preliminary study of thermal comfort in buildings with PV-powered thermoelectric surfaces for radiative cooling. *Energy Procedia* **2017**, *121*, 87–94. [[CrossRef](#)]
27. Irshad, K.; Habib, K.; Thirumalaiswamy, N.; Saha, B.B. Performance analysis of a thermoelectric air duct system for energy-efficient buildings. *Energy* **2015**, *91*, 1009–1017. [[CrossRef](#)]
28. Doi, Y.; Minowa, M.; Uchiyama, M.; Okawa, M.; Kim, K.; Shibui, K.; Kamei, Y. Psychometric assessment of subjective sleep quality using the Japanese version of the Pittsburgh Sleep Quality Index (PSQI-J) in psychiatric disordered and control subjects. *Psychiatry Res.* **2000**, *97*, 165–172. [[CrossRef](#)]
29. Irshad, K.; Algarni, S.; Jamil, B.; Ahmad, M.T.; Khan, M.A. Effect of gender difference on sleeping comfort and building energy utilization: Field study on test chamber with thermoelectric air-cooling system. *Build Environ.* **2019**, *152*, 214–227. [[CrossRef](#)]
30. De Zambotti, M.; Goldstone, A.; Claudatos, S.; Colrain, I.M.; Baker, F.C. A validation study of Fitbit Charge 2TM compared with polysomnography in adults. *Chronobiol. Int.* **2018**, *35*, 465–476. [[CrossRef](#)] [[PubMed](#)]
31. Lee, H.A.; Lee, H.J.; Moon, J.H.; Lee, T.; Kim, M.G.; In, H.; Cho, C.H.; Kim, L. Comparison of wearable activity tracker with actigraphy for sleep evaluation and circadian rest-activity rhythm measurement in healthy young adults. *Psychiatry Investig.* **2017**, *14*, 179–185. [[CrossRef](#)]
32. ISO 15251. *Indoor Environmental Input Parameters for Design and Assessment of Energy Performance of Buildings Addressing Indoor Air Quality, Thermal Environment, Lighting and Acoustics*; ISO: Geneva, Switzerland, 2007.
33. Nicole, F.; Humphreys, M. Derivation of the adaptive equations for thermal comfort in free-running buildings in European standard EN15251. *Build. Environ.* **2010**, *45*, 11–17. [[CrossRef](#)]
34. Humphreys, M.A.; Rijal, H.B.; Nicol, J.F. Updating the adaptive relation between climate and comfort indoors; new insights and an extended database. *Build. Environ.* **2013**, *63*, 40–55. [[CrossRef](#)]
35. Shafie, S.M.; Masjuki, H.H.; Mahlia, T.M.I. Life cycle assessment of rice straw-based power generation in Malaysia. *Energy* **2014**, *70*, 401–410. [[CrossRef](#)]
36. Saidur, R. Energy consumption, energy savings, and emission analysis in Malaysian office buildings. *Energy Policy* **2009**, *37*, 4104–4113. [[CrossRef](#)]
37. Rupp, R.F.; De Dear, R.; Ghisi, E. Field study of mixed-mode office buildings in Southern Brazil using an adaptive thermal comfort framework. *Energy Build.* **2018**, *158*, 1475–1486. [[CrossRef](#)]
38. De Dear, R.; Kim, J.; Parkinson, T. Residential adaptive comfort in a humid subtropical climate—Sydney Australia. *Energy Build.* **2018**, *158*, 1296–1305. [[CrossRef](#)]
39. Mustapa, M.S.; Zaki, S.A.; Rijal, H.B.; Hagishima, A.; Ali, M.S.M. Thermal comfort and occupant adaptive behaviour in Japanese university buildings with free running and cooling mode offices during summer. *Build. Environ.* **2016**, *105*, 332–342. [[CrossRef](#)]
40. Albatayneh, A.; Alterman, D.; Page, A.; Moghtaderi, B. The impact of the thermal comfort models on the prediction of building energy consumption. *Sustainability* **2018**, *10*, 3609. [[CrossRef](#)]
41. Dijk, D.J. Regulation and functional correlates of slow wave sleep. *J. Clin. Sleep Med.* **2009**, *5*, S6. [[PubMed](#)]
42. Allan Hobson, J. A manual of standardized terminology, techniques and scoring system for sleep stages of human subjects. *Electroencephalogr. Clin. Neurophysiol.* **1969**, *26*, 644. [[CrossRef](#)]
43. Vallières, A.; Ivers, H.; Beaulieu-Bonneau, S.; Morin, C.M. Predictability of sleep in patients with insomnia. *Sleep* **2011**, *34*, 609–617. [[CrossRef](#)]

44. Alam, N.; Szymusiak, R.; McGinty, D. Local preoptic/anterior hypothalamic warming alters spontaneous and evoked neuronal activity in the magno-cellular basal forebrain. *Brain Res.* **1995**, *696*, 221–230. [[CrossRef](#)]
45. Heath, M.; Johnston, A.; Dohnt, H.; Short, M.; Gradisar, M. The role of pre-sleep cognitions in adolescent sleep-onset problems. *Sleep Med.* **2018**, *46*, 117–121. [[CrossRef](#)] [[PubMed](#)]
46. Irshad, K.; Habib, K.; Algarni, S.; Saha, B.B.; Jamil, B. Sizing and life-cycle assessment of building integrated thermoelectric air cooling and photovoltaic wall system. *Appl. Therm. Eng.* **2019**, *154*, 302–314. [[CrossRef](#)]
47. Reinikainen, L.M.; Jaakkola, J.J.K. Significance of humidity and temperature on skin and upper airway symptoms. *Indoor Air* **2003**, *13*, 344–352. [[CrossRef](#)] [[PubMed](#)]
48. Schneider, A.; Schuh, A.; Maetzel, F.K.; Rückerl, R.; Breitner, S.; Peters, A. Weather-induced ischemia and arrhythmia in patients undergoing cardiac rehabilitation: Another difference between men and women. *Int. J. Biometeorol.* **2008**, *52*, 535–547. [[CrossRef](#)] [[PubMed](#)]
49. Höpfe, P.; Martinac, I. Indoor climate and air quality. Review of current and future topics in the field of ISB study group 10. *Int. J. Biometeorol.* **1998**, *42*, 1–7.
50. Okamoto-Mizuno, K.; Mizuno, K.; Michie, S.; Maeda, A.; Iizuka, S. Effects of humid heat exposure on human sleep stages and body temperature. *Sleep* **1999**, *22*, 767–773.
51. Tsuzuki, K.; Okamoto-Mizuno, K.; Mizuno, K. Effects of humid heat exposure on sleep, thermoregulation, melatonin, and microclimate. *J. Therm. Biol.* **2004**, *29*, 31–36. [[CrossRef](#)]
52. Lan, L.; Pan, L.; Lian, Z.; Huang, H.; Lin, Y. Experimental study on thermal comfort of sleeping people at different air temperatures. *Build. Environ.* **2014**, *73*, 24–31. [[CrossRef](#)]
53. Strøm-tejsen, P.; Mathiasen, S.; Bach, M.; Petersen, S. The effects of increased bedroom air temperature on sleep and next-day mental performance. In Proceedings of the Proceeding Indoor Air, Ghent, Belgium, 3–8 July 2016.
54. Czeisler, C.A.; Buxton, O.M.; Khalsa, S.B.S. The Human Circadian Timing System and Sleep-Wake Regulation. In *Principles and Practice of Sleep Medicine*; Elsevier, Inc.: Philadelphia, PA, USA, 2005; pp. 375–394, ISBN 9780721607979.
55. Kräuchi, K.; Cajochen, C.; Werth, E.; Wirz-Justice, A. Functional link between distal vasodilation and sleep-onset latency? *Am. J. Physiol. Regul. Integr. Comp. Physiol.* **2000**, *278*, R741–R748. [[CrossRef](#)]
56. Lack, L.; Gradisar, M. Acute finger temperature changes preceding sleep onsets over a 45-h period. *J. Sleep Res.* **2002**, *11*, 275–282. [[CrossRef](#)] [[PubMed](#)]
57. ASHARE. *ASHRAE Standard 55-2010: Thermal Environmental Conditions for Human Occupancy*; American Society of Heating, Refrigerating and Air Conditioning Engineers, Inc.: Atlanta, GA, USA, 2013; p. 58.
58. Somers, V.K.; Dyken, M.E.; Mark, A.L.; Abboud, F.M. Sympathetic-Nerve Activity during Sleep in Normal Subjects. *N. Engl. J. Med.* **1993**, *328*, 303–307. [[CrossRef](#)]



© 2019 by the authors. Licensee MDPI, Basel, Switzerland. This article is an open access article distributed under the terms and conditions of the Creative Commons Attribution (CC BY) license (<http://creativecommons.org/licenses/by/4.0/>).